construction materials

MDPI

Article

From Waste to Performance: Advancing Asphalt Recycling with Waste Oil Rejuvenators

Bushra S. Mankhi [1], Saja A. Sead [1], Noha Shakir Kadhim [1], Zainab Al-Khafaji [2,3], Tameem Mohammed Hashim [4], Mohammed Salah Nasr [5] and Ali Shubbar [6,*]

1 Department of Civil Engineering, College of Engineering, Al-Qasim Green University, Babylon 51013, Iraq; bushra.salman@wrec.uoqasim.edu.iq (B.S.M.)
2 Department of Civil Engineering, Faculty of Engineering and Built Environment, Universiti Kebangsaan Malaysia UKM, Bangi 43600, Selangor, Malaysia
3 Scientific Research Center, Al-Ayen University, Thi-Qar 64001, Iraq
4 Building and Construction Techniques Engineering Department, College of Engineering and Engineering Techniques, Al-Mustaqbal University, Babylon 51001, Iraq
5 College of Engineering, University of Babylon, Babylon 51005, Iraq; eng511.mohammed.nasr@uobabylon.edu.iq
6 School of Civil Engineering and Built Environment, Liverpool John Moores University, Liverpool L3 5UX, UK
* Correspondence: a.a.shubbar@ljmu.ac.uk

Abstract

The growing use of reclaimed asphalt pavement (RAP) in hot mix asphalt (HMA) is an important practice to achieve more sustainable pavements, as it reduces the consumption and environmental impact of virgin materials. However, aging induces binder stiffening that requires effective rejuvenation to restore overall performance. This study provides a comprehensive comparative analysis of ten chemically different waste oils—waste engine oil (WEO), waste cooking oil (WCO), yellow grease (YG), waste hydraulic oil (WHO) waste electric transformer oil (WETO), slop oil (SO), sludge-derived bio-oil (SDBO), tire pyrolysis oil (TPO), plastic pyrolysis oil (PPO), and algal residue oil (ARO)—as recycled HMA mixture rejuvenators, linking oil composition to binder regeneration and mixture performance. Binder properties were determined by rotational viscosity (RV), dynamic shear rheometer (DSR) and bending beam rheometer (BBR), whereas mixture performance was assessed in terms of Superpave mechanical properties, Hamburg wheel-tracking test (HWTT) for rutting resistance and mixture BBR for low-temperature cracking resistance. Performance grade (PG) evaluations showed that WETO and WEO restored the 50% and 75% RAP binders, respectively, to a grade close to PG 64-16 at the lowest dosages. The Superpave volumetric properties of all restored mixtures were similar to those of the control mixture, denoting corrected mixture balance and compaction level. HWTT results indicated that WETO-recycled mixtures revealed the lowest rut depth at 50% RAP, while WEO-recycled mixtures exhibited the lowest rut depth at 75% RAP after 20000 passes. Additional evidence supporting these results can be found in BBR mixture data, which demonstrated that WETO at 50% RAP and WEO/WETO at 75% RAP showed the most reduction in creep stiffness and improvement in creep rate. The correlation, regression, and PI analyses were in good agreement with the experimental results, where WETO and WEO exhibited the best overall performance at 50% and 75% RAP, respectively. In summary, these results indicate that the performance of waste oil rejuvenator in recycled HMA mixtures is highly dependent on RAP content and point to WETO and WEO as feasible, environmentally friendly options for high-RAP recycled HMA.

Received: 17 May 2026
Revised: 11 June 2026
Accepted: 16 June 2026
Published: 26 June 2026

Keywords: reclaimed asphalt pavement (RAP); waste oil rejuvenators; sustainable asphalt mixtures; low-temperature cracking

1. Introduction

1.1. Research Background

With the demand for sustainable, cost-effective and high-performance replacements to traditional additives being sought after by the pavement industry, the use of waste oils in HMA technology has gained a significant amount of preference [1]. As the use of RAP continues to increase, and the world continues to push for less reliance on virgin petroleum sources, waste oils present themselves as a viable modifier and rejuvenator that can restore aged binder characteristics, improve the workability of mixture, and improve the long-term durability of the pavement [2].

A significant number of waste oils obtained from various industrial or domestic waste streams has been studied for use as asphalt modifiers. These include WEO, WCO [3], waste animal fat oil, YG [4], WHO [5], WTO [6], diesel storage sludge oil (SO) [7], SDBO [8], TPO [9], PPO [10], and ARO [11]. Although they have some common characteristics, each of these waste oils has its own chemical composition and each contains different amounts of aromatics, fatty acids, phenolics and oxygenated compounds that will affect their behavior when interacting with asphalt coats [4]. It has been proved by research that adding these waste oils in HMA could effectively decrease the viscosity of the binder, lower the mixing and compaction temperature, recover the colloidal balance of aged asphalt and enhance the anti-cracking performance and resistance to oxidation aging [5]. Some of these additives, like TPO and PPO, add further benefits regarding elastic behavior and high-temperature performance since they are aromatic rich [9,10]. Still others, such as WCO and WEO, have high rejuvenating properties, which make them suitable for RAP-rich mixes [3]. Beside their engineering advantages, the use of waste oils is also in accordance with circular economy principles as they enable large volumes of waste to be redirected from disposal streams and converted into useful materials for infrastructure [7]. With growing environmental restriction and increasing sustainability goals, the introduction of waste oils into asphalt mixtures becomes a feasible, scalable and greenable alternative for contemporary pavement engineering [12]. This paper investigates the properties, mechanism, and effect on practice of various types of waste oils used as regenerators in recycled HMA. The character of binder behavior is evaluated by DSR, BBR, and RV test methods. Mixture performance is characterized based on Superpave mechanical properties, the wheel-tracking test for rutting resistance and the BBR test of the HMA with regard to low-temperature cracking susceptibility through creep stiffness and creep rate. Furthermore, correlation, regression, and PI analyses were performed to provide additional insight into the results.

1.2. Literature Review

Waste oils show good performance in improving the engineering properties of recycled HMA mixes. Studies have consistently demonstrated that various types of waste oils can rejuvenate aged binders in RAP to enhance workability and restore flexibility by improving fatigue and low-temperature cracking resistance. Although a variety of different categories of waste oils might still be used to maintain rutting resistance, specifically the ones with high aromatic content could show great potential for rejuvenating aged binders effectively.

Li et al. [13] found that adding WEO combined with carbon nanotubes can greatly enhance the performance of RAP mixture such as improving rutting resistance, low-temperature cracking resistance and Marshall stability to a level similar to that of con-

ventional mixtures. They concentrate on the synergistic effect of one waste oil which is reinforced by nanomaterial. On the other hand, the present study extends this work by comparing several waste oils without additional modifiers, providing a clearer assessment of their rejuvenation effectiveness in high-RAP mixtures.

Jain [14] characterized the properties of recycled asphalt mixes with WCO as an only source rejuvenator and reported significant improvements in workability, fatigue performance and overall environmental impact due to less dependence on the virgin binder. The research focuses on the successful use of WCO as rejuvenator to restore aged binder properties in RAP mixtures with tangible sustainable benefits. The current study takes a more comprehensive approach by evaluating various waste oil sources instead of one source, providing a broader performance comparison, and evaluating the relative effectiveness of different waste oils as rejuvenators for recycled HMA mixtures.

Bilema et al. [15] studied the recycled asphalt mixture modified by waste frying oil (WFO) and crumb rubber, and concluded that obvious enhancements in the flexibility, fatigue performance and Marshall strength could be attributed to the combined effect of rejuvenating and elastic property of additives. Their findings indicate that the utilization of WFO, for counteracting the aging effects and CR, to improve the mechanical properties of RAP mixtures is a feasible alternative. By contrast, the present study aims to examine the effect of rubber-free waste oils only, enabling a direct comparison among a wider range of waste oil sources and facilitating the identification of the most effective rejuvenator for recycled HMA mixtures.

Khan et al. [16] studied high-RAP mixtures containing waste engine oil (WEO) as a rejuvenator and crumb rubber as a modifier. They reported significant improvements in mixture strength, fatigue life, and rutting resistance, which were attributed to the combined softening effect of WEO and the elastic contribution of crumb rubber. Their findings confirmed that WEO can effectively restore aged binder properties in high-RAP mixtures; however, the individual effect of the waste oil could not be separated from that of crumb rubber. By contrast, the present study focuses on the rejuvenation efficiency of various waste oils without crumb rubber, allowing a broader comparison of waste oil sources and their suitability for RAP hot mix asphalt applications. Furthermore, Zhao et al. [17] investigated the possibility of using a palmitamide obtained from waste edible oil as WMA additive, and found that it was able to provide an improved workability, reduced mixing and compaction temperatures as well as acceptable mechanical performances, which means that the waste-derived palmitamide was efficient in improving the performance of WMA with less energy consumption. Their results show that by recycling waste cooking oil into valuable materials, the development of new asphalt modifiers can be a win-win process in terms of both performance and plant operation. With an interest in diverse waste oil characterization, the current research focuses on assessing rejuvenation in recycled HMA mixtures with various types of waste oils rather than one produced additive so that comparison can be made among different waste oil sources to identify the most effective rejuvenator for RAP-based mixtures.

Jain S, and Chandrappa AK [18] reported that WCO improved binder blending and restored the properties of recycled mixtures with high content of RAP. However, their study was limited to a single rejuvenator source. In contrast, the present study provides a comprehensive comparison of ten chemically distinct waste oils from industrial, domestic, and biogenic origins, offering a broader understanding of how waste oil composition influences binder regeneration and the performance of recycled HMA mixtures. Likewise, Liu F et al. [19] showed that asphalt binders rejuvenated with WEO gradually regained stiffness during the re-aging process, emphasizing the importance of long-term durability. While their study focused on the aging behavior of a single rejuvenator, the current work

demonstrates that different waste oils exhibit varying abilities to restore aged binder properties, suggesting that waste oil composition also influence the long-term aging response of rejuvenated RAP mixtures. In addition, Tushar Q et al. [20] highlighted the environmental benefits of using WCO as a rejuvenator in high-RAP mixtures, demonstrating reduced emissions and lower consumption of virgin materials. However, their conclusions were based on a single rejuvenator type. By considering waste oils from different sources, the present study provides a more comprehensive understanding of their influence on binder restoration and recycled HMA performance.

1.3. The Novelty of the Study

This work provides a comprehensive comparative assessment of ten chemically distinct waste oils, viz., WEO, WCO, YG (waste animal fat), WHO (waste hydraulic oil), WETO (waste electric transformer oil), SO (diesel storage/sludge oil), SDBO (sludge derived bio-oil), TPO (tire pyrolysis oil), PPO (plastic pyrolysis oil), and ARO (algal residue), as binder rejuvenators for recycled HMA mixtures. In addition, the study explores the direct relationship between the composition of the used oils, the regeneration mechanisms of the binder, and the performance of resulting mixture, as illustrated in Figure 1. This work expands current knowledge by evaluating waste oils from industrial, domestic, and biogenic sources and assessing their potential as sustainable alternatives for producing high-performance recycled asphalt mixtures. Furthermore, correlation, regression, and PI analyses are incorporated to provide a quantitative comparison of rejuvenator performance.

Figure 1. Waste oil rejuvenation process in recycled HMA.

1.4. The Objectives of the Study

The aim of this study is to evaluate the rejuvenation potential of ten chemically different waste oils in recycled HMA mixtures by correlating their composition with binder recovery and mechanical properties. Binder properties are evaluated by the RV, DSR, and BBR tests, and the performance of the mixtures is determined based on Superpave parameters, the wheel-tracking test (rutting), and the BBR test for low-temperature cracking susceptibility. In addition, statistical analyses are employed to further examine the performance of the investigated rejuvenators. The ultimate purpose is to find out what kind of waste oil can provide the best regeneration and highest performance for RAP mixtures.

2. Experimental Program

2.1. Materials and Rejuvenators

Ordinary local construction materials were used in the current study, including virgin aggregate and binder, in addition to waste materials (RAP and waste oils). Prior to use, the RAP material was oven-dried and screened to obtain the required gradation, while the collected waste oils were filtered to remove suspended impurities and solid particles.

2.1.1. Virgin Asphalt Binder

The use of PG 64-16 asphalt (Al-Hilla, Babil, Iraq) binder was used because it is a product that fits well in high-temperature areas with heavy load traffic due to its stiffness and excellent resistance to rutting. This binder type has been implemented in HMA mixtures to enhance resistance against aging, reduce permanent deformation and retain mixture stability, especially in high-temperature zones of heavy loading. The point of grade is a property determined in the binder PG 64-16 according to Superpave specifications based on performance as in Table 1 below. Figures 2–5 present the characterization test apparatus applied in the current study such as DSR (manufactured by Brookfield Engineering Laboratories (AMETEK), Middleboro, MA, USA), rotatory rheometer (manufactured by Brookfield Engineering Laboratories, Inc., Middleboro, MA, USA), pressure aging vessel (PAV) (manufactures by Infratest Prüftechnik GmbH, Brackenheim, Baden-Württemberg, Germany) and BBR (manufactures by Applied Test Systems (ATS), Butler, PA, USA) which were used to measure the bitumen properties.

Table 1. The key physical characteristics of PG 64-16 bitumen.

Test Property	The Result	Standard	Requirement
Performance Grade (PG)	PG 64-16	AASHTO M320 [21]	PG 64-16
High Pavement Temperature	64 °C	AASHTO T315 (DSR) [22]	64 °C
Low Pavement Temperature	−16 °C	AASHTO T313 (BBR) [23]	−16 °C
Viscosity at 135 °C	2.1 Pa·s	AASHTO T316 [24]	≤3.0 Pa·s
DSR G*/sin δ (Unaged Binder)	1.20 kPa	AASHTO T315 [22]	≥1.00 kPa
DSR G*/sin δ (RTFO-aged Binder)	2.5 kPa	AASHTO T315 [22]	≥2.20 kPa
G*·sin δ (PAV-aged Binder)	3500 kPa	AASHTO T315 [22]	≤5000 kPa
BBR Stiffness (S) at −16 °C	260 MPa	AASHTO T313 [23]	≤300 MPa
Flash Point	240 °C	AASHTO T48 [25]	≥230 °C
Solubility in Trichloroethylene	99.7%	AASHTO T44 [26]	≥99%

Figure 2. Brookfield rotational.

Figure 3. Bending beam rheometer viscometer.

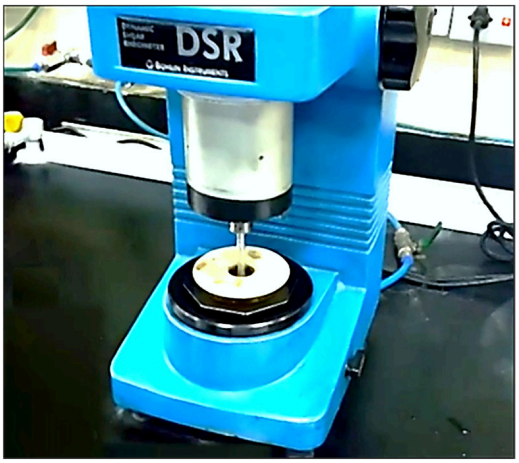

Figure 4. Dynamic shear rheometer.

Figure 5. Pressure aging vessel.

2.1.2. The Aggregate Utilized in the Study

In Iraq, the main source of coarse aggregate are crushed stones from nearby quarries and crushed limestone is the most widely used for this purpose due to its availability and good mechanical properties. Fine aggregate is normally river sand, with some adjustment in gradation and impurities. Coarse aggregate: Crushed stone is used through concrete, grounds and works of the asphalt in all parts of Iraq. Natural sand is used as fine aggregate.

These materials meet a grading, cleanliness and strength requirement according to the Iraqi specification for roads and bridges (SORB 2009) [27] and they have successful performance under local conditions. The physical properties of the coarse and fine aggregate used are shown in Tables 2 and 3.

The upper layer (wearing course) aggregate gradation was designed based on the Iraqi SORB, where the middle of a 12.5 mm nominal maximum aggregate size (NMAS) was adopted. The proposed gradation is within the SORB limits for each sieve size, and results in a dense ensure (well grade) structure, with good particle interlock, stability, rutting under local traffic and climate conditions. This gradation would also promote adequate compaction and good adhesion of the aggregate to the asphalt binder in hot climates as illustrated by Table 4.

Table 2. The physical characteristics of the selected coarse aggregate.

Test Property	Bulk Specific Gravity, Gsb	Apparent Specific Gravity, Gsa	Water Absorption	Los Angeles Abrasion Loss	Elongation Index
The Result	2.62	2.78	1.4%	23%	26%
Standard	ASTM C127 [28]	ASTM C127 [28]	ASTM C127 [28]	ASTM C131 [29]	ASTM D4791 [30]
Requirement	2.60–2.75	2.70–2.85	<2.0%	≤30%	≤30%

Table 3. The physical characteristics of the selected fine aggregate.

Test Property	Bulk Specific Gravity, Gsb	Apparent Specific Gravity, Gsa	Water Absorption	Sand Equivalent Value	Fineness Modulus
The Result	2.62	2.78	1.4%	23%	26%
Standard	ASTM C128 [31]	ASTM C128 [31]	ASTM C128 [31]	ASTM D2419 [32]	ASTM C136 [33]
Requirement	2.60–2.70	2.70–2.85	<1.5%	≥45%	2.3–3.1

Table 4. Surface layer aggregate gradation.

Sieve Size (mm)	Specification (%)	Middle Specification (%)
19.0 mm	100	100
12.5 mm (NAMS)	90–100	95
9.5 mm	75–85	80
4.75 mm	35–45	40
2.36 mm	22–30	26
0.30 mm	12–18	15
0.075 mm	6–10	8

2.1.3. The Utilized Filler

Portland cement was used as a mineral filler in HMA to increase the stiffness of mixture, resistant against moisture damage and overall durability under traffic loading. It is a physical and economical alternative for traditional fillers. The physical properties of Portland cement are shown in Table 5.

Table 5. The physical properties of the filler used [34].

Test Property	Specific Gravity	Blaine Fineness (Surface Area)
The Result	3.15	350 m^2/kg
Standard	ASTM C188 [35]	ASTM C204 [36]
Requirement	3.10–3.20	≥280 m^2/kg

2.1.4. Reclaimed Asphalt Pavement (RAP)

RAP was incorporated into the HMA mixtures as a sustainable source of aggregates and aged binder. The use of RAP reduces the demand for virgin materials and lowers overall production costs while supporting environmental conservation. Prior to mixing, the RAP stockpile, as shown below in Figure 6, was thoroughly homogenized, and the physical properties of the recovered materials were determined to ensure uniformity and consistent quality, as shown below in Tables 6 and 7. The processed RAP was then blended with virgin aggregates and fresh binder according to the target mixture design requirements [37].

Figure 6. RAP stockpile before homogenization.

Table 6. The physical properties of the recovered RAP binder.

Test Property	The Result	Standard
Recovery Method	Solvent extraction and recovery	AASHTO T164/T319 [38]
Binder Content (% of RAP)	3.9%	AASHTO T164 [39]
Penetration (25 °C, 0.1 mm)	12	AASHTO T49 [40]
Softening Point (°C)	75 °C	AASHTO T53 [41]
Dynamic Viscosity at 135 °C (Pa·s)	3.2	AASHTO T316 [24]
DSR G*/sin δ	4.5 kPa	AASHTO T315 [22]
Performance Grade	PG 76-10	AASHTO M320 [21]

Table 7. The physical properties of the recovered RAP aggregates.

Test Property	The Result	Standard
Bulk Specific Gravity, Gsb	2.50	AASHTO T84/T85 [42]
Apparent Specific Gravity, Gsa	2.65	AASHTO T84/T85 [42]
Absorption (%)	2.0%	AASHTO T85 [42]
Fines Content (Passing 0.075 mm, %)	8%	AASHTO T27/T11 [43]
LA Abrasion Loss (%)	26%	AASHTO T96 [44]
Sand Equivalent (%)	60%	AASHTO T176 [45]
Flakiness Index (%)	15%	ASTM D4791 [30]

The recovered RAP aggregates were obtained through a standard binder extraction procedure in accordance with the relevant specifications. After completing the extraction process, the aggregates were subjected to a sieve analysis to determine their particle size distribution. This approach allows the gradation of the RAP material to be evaluated in its in-service condition after long-term field aging [46]. The gradation of the recovered aggregates obtained from the sieve analysis is presented in Table 8.

Table 8. Recovered aggregate gradation.

Sieve Size (mm)	Recovered Gradation (%)
9.0 mm	100
12.5 mm (NAMS)	96
9.5 mm	82
4.75 mm	42
2.36 mm	28
0.30 mm	17
0.075 mm	10

2.1.5. Waste Engine Oil (WEO)

WEO was chosen as a rejuvenator to be added into the HMA mix in order for the aged properties of the binder present in RAP materials to be brought back. The WEO employed in this work was retrieved from a local automobile workshop, which is an accessible and less expensive waste stream, and is shown below in Figure 7. Its chemical composition (content of light hydrocarbons and maltenes-like fractions) has been shown to improve the flexibility of a binder and decrease its stiffness resulting from long-term aging [3]. Its key physical properties are summarized in Table 9.

Figure 7. WEO sample.

Table 9. The physical properties of the used WEO.

Test Property	The Result	Standard
Density at 25 °C (g/cm^3)	0.885	ASTM D4052 [47]
Kinematic Viscosity at 100 °C (cSt)	10.0	ASTM D445 [48]
Flash Point (°C)	200	ASTM D92 [49]
Pour Point (°C)	−18	ASTM D97 [50]
Water Content (%)	0.15	ASTM D95 [51]

2.1.6. Waste Cooking Oil (WCO)

WCO was then used in the HMA mix as an eco-friendly bio-rejuvenator for restoring the rheological equilibrium of an aged asphalt binder in RAP. The WCO employed in the present study was sourced from local eateries to simulate a convenient source of waste produced on high yield scale with low processing requirement. The oxidized binder can be softened by the high content of natural fatty and triglycerides in WCO, thus improving low-temperature performance [3] (see Figure 8 below) and promoting the workability of the mixture. The physical properties of the used WCO are listed in Table 10.

Figure 8. WCO sample.

Table 10. The physical properties of the used WCO.

Test Property	The Result	Standard
Density at 25 °C (g/cm^3)	0.915	ASTM D4052 [47]
Kinematic Viscosity at 100 °C (cSt)	7.0	ASTM D445 [48]
Flash Point (°C)	260	ASTM D92 [49]
Pour Point (°C)	−5	ASTM D97 [50]
Water Content (%)	0.20	ASTM D95 [51]

2.1.7. Waste Animal Fat Oil (Yellow Grease, YG)

YG, also known as waste animal fat oil, was collected from local food-processing and restaurant sources and evaluated as a rejuvenator for RAP-based HMA mixtures, as shown in Figure 9. The oil is rich in long-chain saturated fatty acids and thermal degradation products, which can reduce stiffness in aged asphalt binder and enhance low-temperature performance [4]. The main physical properties of the YG sample used in this study are summarized below in Table 11.

Figure 9. YG sample.

Table 11. The physical properties of the used YG.

Test Property	The Result	Standard
Density at 25 °C (g/cm^3)	0.925	ASTM D4052 [47]
Kinematic Viscosity at 100 °C (cSt)	8.5	ASTM D445 [48]
Flash Point (°C)	240	ASTM D92 [49]
Pour Point (°C)	−3	ASTM D97 [50]
Water Content (%)	0.30	ASTM D95 [51]

2.1.8. Waste Hydraulic Oil (WHO)

WHO was obtained from local mechanical workshops as an industrial lubricant waste, as shown in Figure 10. Due to its mineral base oil structure and stable viscosity profile, WHO was evaluated as a potential rejuvenating agent for aged asphalt binder within RAP mixtures [5]. The physical properties of the collected WHO sample were characterized according to standardized ASTM procedures and are presented in Table 12.

Figure 10. WHO sample.

Table 12. The physical properties of the used WHO.

Test Property	The Result	Standard
Density at 25 °C (g/cm^3)	0.870	ASTM D4052 [47]
Kinematic Viscosity at 100 °C (cSt)	6.8	ASTM D445 [48]
Flash Point (°C)	210	ASTM D92 [49]
Pour Point (°C)	−12	ASTM D97 [50]
Water Content (%)	0.10	ASTM D95 [51]

2.1.9. Waste Electric Transformer Oil (WETO)

WETO was collected from local electrical maintenance workshops and evaluated as a rejuvenator agent for aged asphalt binder within RAP-based HMA mixtures, as shown in Figure 11. The used oil contains degraded mineral base stock enriched with light hydrocarbon fractions formed through long-term thermal and electrical aging, which can soften oxidized binder and improve low-temperature performance [6]. Using WETO supports resource recovery from an industrial waste stream, reduces disposal impacts, and promotes sustainable asphalt production. The main physical properties of the WETO sample are summarized in Table 13.

Figure 11. WETO sample.

Table 13. The physical properties of the used WETO.

Test Property	The Result	Standard
Density at 25 °C (g/cm^3)	0.890	ASTM D4052 [47]
Kinematic Viscosity at 100 °C (cSt)	4.3	ASTM D445 [48]
Flash Point (°C)	155	ASTM D92 [49]
Pour Point (°C)	−30	ASTM D97 [50]
Water Content (%)	0.03	ASTM D95 [51]

2.1.10. Diesel Storage Sludge Oil (Slop Oil, SO)

Slop oil (SO) was collected from the waste sludge produced during diesel storage at local fuel stations, as shown in Figure 12. The material represents a complex waste mixture of heavy hydrocarbons, oxidized residues, water and sediments formed through long-term storage and fuel degradation [7]. Due to its high viscosity and elevated content of light diesel fractions, SO was employed as a rejuvenator agent for aged asphalt binders in RAP mixtures. The main physical properties of the SO sample used in this study are summarized in Table 14.

Figure 12. SO sample.

Table 14. The physical properties of the used SO.

Test Property	The Result	Standard
Density at 25 °C (g/cm^3)	0.955	ASTM D4052 [47]
Kinematic Viscosity at 100 °C (cSt)	12.5	ASTM D445 [48]
Flash Point (°C)	90	ASTM D92 [49]
Pour Point (°C)	+5	ASTM D97 [50]
Water Content (%)	8.0	ASTM D95 [51]

2.1.11. Sludge-Derived Bio-Oil (SDBO)

SDBO was produced from the thermochemical conversion of municipal sewage sludge collected from local wastewater treatment stations, as shown in Figure 13. The resulting bio-oil is rich in oxygenated organic compounds and aromatic fractions, which can soften aged asphalt binder and improve the ductility of RAP-based mixtures [8]. Using SDBO as a rejuvenator promotes circular resource use, reduces the environmental impact of sludge disposal, and introduces a renewable component into asphalt production. The physical properties of the SDBO sample are summarized in Table 15.

Figure 13. SDBO sample.

Table 15. The physical properties of the used SDBO.

Test Property	The Result	Standard
Density at 25 °C (g/cm^3)	1.05	ASTM D4052 [47]
Kinematic Viscosity at 100 °C (cSt)	17.5	ASTM D445 [48]
Flash Point (°C)	78	ASTM D92 [49]
Pour Point (°C)	−10	ASTM D97 [50]
Water Content (%)	22.0	ASTM D95 [51]

2.1.12. Tire Pyrolysis Oil (TPO)

TPO was obtained from the thermochemical conversion of end-of-life tires in a local pyrolysis facility, representing a hydrocarbon-rich waste stream suitable for asphalt rejuvenation, as shown in Figure 14. It is a product obtained by condensing the oil gas decomposed during the high-temperature process, resulting in an oil composed mainly of light and medium aromatics with minimal water content. Such characteristics enable TPO to effectively soften oxidized RAP binder and improve low-temperature ductility [9]. The main physical properties of the TPO sample are summarized in Table 16.

Figure 14. TPO sample.

Table 16. The physical properties of the used TPO.

Test Property	The Result	Standard
Density at 25 °C (g/cm^3)	0.945	ASTM D4052 [47]
Kinematic Viscosity at 100 °C (cSt)	4.8	ASTM D445 [48]
Flash Point (°C)	62	ASTM D92 [49]
Pour Point (°C)	−24	ASTM D97 [50]
Water Content (%)	0.5	ASTM D95 [51]

2.1.13. Plastic Pyrolysis Oil (PPO)

PPO was obtained from the thermochemical conversion of waste plastic feedstocks in a local pyrolysis facility, representing a hydrocarbon-rich liquid suitable for asphalt rejuvenation, as shown in Figure 15. It is a product formed by condensing the vapor-phase hydrocarbons released during the high-temperature cracking of plastics in an oxygen-free reactor. The resulting oil is predominantly composed of saturated and unsaturated aliphatic hydrocarbons with low water content, enabling effective softening of oxidized RAP binder and enhancing mixture workability [10]. The main physical properties of the PPO sample are summarized in Table 17.

Figure 15. PPO sample.

Table 17. The physical properties of the used PPO.

Test Property	The Result	Standard
Density at 25 °C (g/cm^3)	0.830	ASTM D4052 [47]
Kinematic Viscosity at 100 °C (cSt)	1.6	ASTM D445 [48]
Flash Point (°C)	28	ASTM D92 [49]
Pour Point (°C)	−30	ASTM D97 [50]
Water Content (%)	0.10	ASTM D95 [51]

2.1.14. Algal Residue Oil (ARO)

ARO was obtained from the thermochemical conversion of residual microalgae biomass collected after primary lipid extraction for biodiesel production, as shown in Figure 16. The oil is formed by condensing the volatile organic compounds released during high-temperature liquefaction of algal residues in an oxygen-limited reactor. ARO contains a mixture of long-chain fatty acids, oxygenated aromatics, and heterocyclic compounds, which can soften oxidized RAP binder and improve low-temperature flexibility when used as a bio-based rejuvenator [11]. Incorporating ARO into HMA supports circular utilization of algal waste, adds value to biodiesel by-products, and reduces disposal impacts. The main physical properties of the ARO sample used in this study are summarized in Table 18.

Figure 16. ARO sample.

Table 18. The physical properties of the used ARO.

Test Property	The Result	Standard
Density at 25 °C (g/cm^3)	1.02	ASTM D4052 [47]
Kinematic Viscosity at 100 °C (cSt)	18.0	ASTM D445 [48]
Flash Point (°C)	112	ASTM D92 [49]
Pour Point (°C)	−6	ASTM D97 [50]
Water Content (%)	18.0	ASTM D95 [51]

2.2. In-Depth Laboratory Analysis

2.2.1. Control HMA Mixture

The mixing and compaction temperatures (MTCs) for the control mixture were determined using the rotational viscometer (RV) test in accordance with AASHTO T316. In this procedure, approximately 11 g of bitumen is heated and tested using a cylindrical spindle rotating at 20 rpm to measure the binder's viscosity at various temperatures. Measurements were conducted between 135 °C and 175 °C, and the resulting viscosity values (Pa·s) were plotted against temperature to establish the viscosity–temperature relationship. Based on Superpave viscosity limits, the PG 64-16 control binder reached the required viscosities for mixing (0.17 Pa·s) and compaction (0.28 Pa·s) at 165 °C and 150 °C, respectively, providing suitable workability and compaction performance, as illustrated in Figure 17.

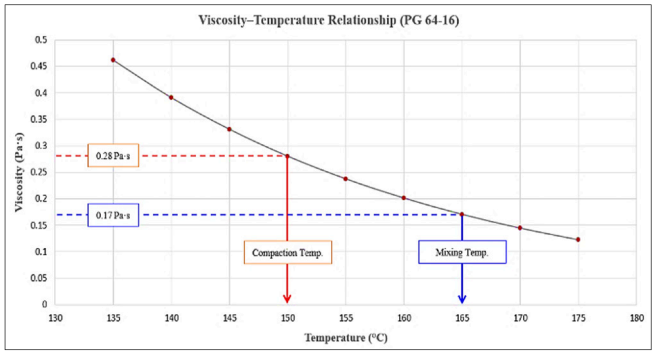

Figure 17. Viscosity–temperature relationship (PG 64-16).

The optimum bitumen content (OBC) for the control mixture was established following the Superpave design approach outlined in AASHTO R35 [52]. Trial batches were produced at four asphalt contents (5.5%, 6.0%, 6.5%, and 7.0%), three asphalt specimens for each content, and their volumetric characteristics were evaluated. The binder content that achieved the design air-void level of 4.0% was adopted as the OBC, which corresponded to 4.8%. All the specimens were compacted using the Superpave Gyratory Compactor (SGC), as illustrated in Figure 18.

2.2.2. Recycled Mixtures

The RAP contents used in the mixtures were 25%, 50%, and 75% by total mixture weight. The total binder content was kept equal to the optimum binder content of the control mix. The effective contribution of the RAP binder was calculated from the measured RAP binder content and the selected RAP percentage in the mixture, and the virgin binder content was reduced accordingly. The required virgin binder content was obtained from Equation (1) below.

$$P_{b,virgin} = P_{b,target} - \left(P_{RAP} \times B_{RAP} \times K_1\right) \quad (1)$$

$P_{b,virgin}$: optimum binder for control mix (4.8%).

$P_{b,target}$: the target total binder content.
P_{RAP}: the RAP proportion in the mix.
B_{RAP}: the RAP binder content (3.9%).
K_1: activity factor of the RAP binder (taken as 1.0 in this study, meaning that all the aged binder in the RAP was considered available to interact with and contribute to the effective binder content of the mixture) [53].

Figure 18. Compaction equipment.

The required virgin binder at each RAP level was calculated using Equation (1) and is presented in Table 19 below.

Table 19. Binder contribution at different RAP levels.

RAP %	P_{RAP}	RAP Binder (%)	Virgin Binder (%)	Total Binder (%)
25%	0.25	0.975%	3.825%	
50%	0.50	1.950%	2.850%	4.8%
75%	0.75	2.925%	1.875%	

The effective PG of the blended binder in the recycled mixtures was determined using DSR and BBR testing, as shown in Figures 19 and 20, considering the high and low temperature performance grades of the virgin binder (PG 64-16) and the extracted RAP binder (PG 76-10) weighted according to their proportions in the total binder content.

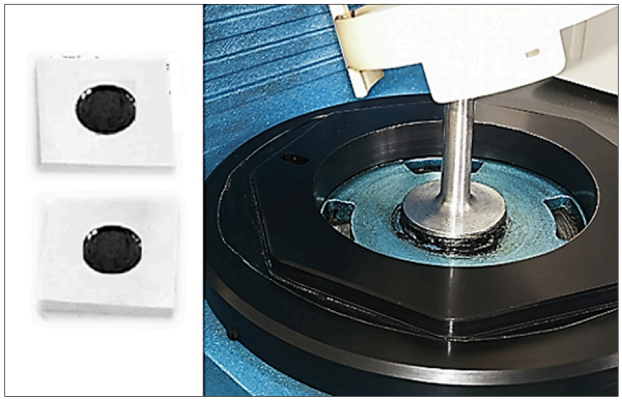

Figure 19. DSR testing procedure.

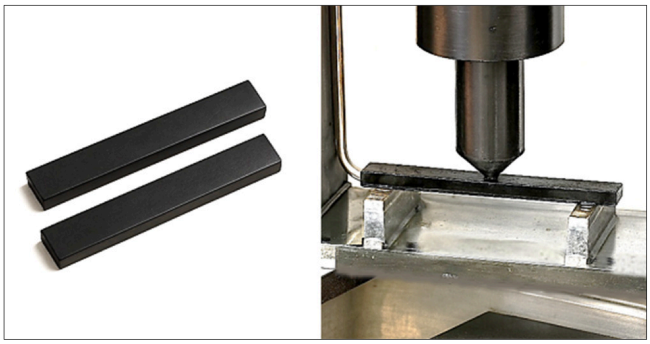

Figure 20. BBR testing procedure.

The blended binders (virgin and aged RAP binder) corresponding to each RAP level were evaluated to determine their effective performance grade, and the results are summarized in Table 20.

Table 20. PG of virgin–RAP binder blends.

RAP%	Binder Blend	Temp. (High)	Temp. (Low)	PG
25%	20% RAP binder + 80% virgin binder	66.4 °C	−14.8 °C	PG 64-16
50%	41% RAP binder + 59% virgin binder	68.9 °C	−13.6 °C	PG 70-16
75%	61% RAP binder + 39% virgin binder	71.3 °C	−12.3 °C	PG 70-10

2.2.3. Rejuvenated Mixtures

Ten types of waste oils were used to rejuvenate the aged characteristics of RAP in the HMA mixtures. However, at 25% RAP, the resulting binder blend was similar to the virgin binder; therefore, no rejuvenation was required for this RAP level. Several dosages of the used rejuvenators were used after multiple lab trials at each RAP percentage. The optimum dosage was selected as the minimum amount required to restore the blended binder performance grade from PG 70-16 and PG 70-10 to the target grade of PG 64-16, as summarized in Table 21 below.

Table 21. Rejuvenator dosage ranges for PG restoration of blended binders.

Rejuvenated Blend	Trial Range of Rejuvenators
WEO + Blend of 50% RAP	4–9%
WEO + Blend of 75% RAP	5–10%
WCO + Blend of 50% RAP	6–11%
WCO + Blend of 75% RAP	10–15%
YG + Blend of 50% RAP	5–10%
YG + Blend of 75% RAP	8–15%
WHO + Blend of 50% RAP	3–8%
WHO + Blend of 75% RAP	6–11%
WETO + Blend of 50% RAP	2–7%
WETO + Blend of 75% RAP	5–12%
SO + Blend of 50% RAP	4–9%
SO + Blend of 75% RAP	7–14%
SDBO + Blend of 50% RAP	7–13%
SDBO + Blend of 75% RAP	10–19%
TPO + Blend of 50% RAP	6–11%
TPO + Blend of 75% RAP	9–15%
PPO + Blend of 50% RAP	5–10%
PPO + Blend of 75% RAP	7–13%
ARO + Blend of 50% RAP	9–14%
ARO + Blend of 75% RAP	12–19%

It should be noted that the dosage was selected based on binder performance grade restoration, while the mixture performance tests were carried out afterward to assess the effectiveness of the selected dosage. The mixing and compaction temperatures of the recycled and rejuvenated mixtures were maintained to be similar to those of the control mixture to ensure a consistent and unbiased comparison. This approach isolates the effects of RAP and rejuvenators from temperature influences, reflects practical field conditions, and avoids excessive heating that could accelerate binder aging or distort mixture performance.

The virgin binder was heated to the target mixing temp. of 165 °C and blended with the predetermined amount of waste oil rejuvenator using a high-shear mixer operating (manufactured by Siemens AG, Munich, Germany) at 3000 rpm for 30 min to ensure a homogeneous blend as shown in Figure 21.

Figure 21. High shear binder mixer.

RAP and virgin aggregates were heated separately to the target mixing temperature and then combined according to the designed mixture. The rejuvenated binder was then added to the aggregate blend and mixed for 2 to 3 min using a mechanical mixing machine (manufactured by Controls S.p.A., Liscate, Italy) as shown in Figure 22, until complete coating of all particles was achieved. The recycled mixtures were then compacted at the designated compaction temperature at 150 °C using the SGC (manufactured by Controls S.p.A., Liscate, Italy) in accordance with the AASHTO T312 [54] at the design number of gyrations (N_{design} = 100) corresponding to a highway traffic level of 3 to 30 million ESALs, which is consistent with the SORB requirements for heavy traffic in Iraq.

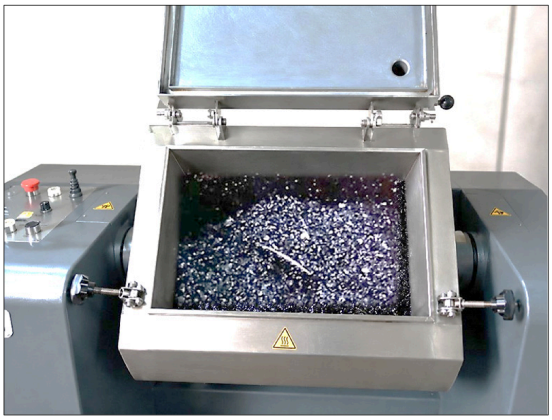

Figure 22. Mechanical mixer of asphalt.

2.3. Performance Assessment

2.3.1. Superpave Characteristics

Volumetric properties of Superpave are the primary factors reflecting the HMA quality and performance under service conditions. These traits are air voids (Va), void in mineral aggregate (VMA) and void filled with asphalt (VFA), measured following the AASHTO R35 and AASHTO M323 [55], by preparing three specimens for each mix. For dense-graded HMA mixes, air voids should be kept at about 3–5% and VMA adequacy to applicable NMS in use; VFA expectations are typically between 65 and 75%. Meeting these volumetric requirements will provide sufficient strength and resistance to plastic deformation, as well as adequate binder content for long-term performance.

2.3.2. Hamburg Wheel-Tracking Test (HWTT)

The HWTT, carried out in accordance with AASHTO T324 [56], is a reliable test to measure the rutting and moisture susceptibility of hot mix asphalt (HMA) mixtures. In this test, two cylindrical samples having a nominal size of 150 mm in diameter and 62 ± 2 mm in height are put into a water bath with the temperature control system at 50 °C as shown in Figure 23. Densification of the labs is done using the Superpave Gyratory Compactor in accordance with AASHTO T312 [54], for consistent density and air-void levels. A steel wheel with a repeating load of 705 N is traversed on the sample surface for up to 20,000 passes with rut depth recorded throughout the process.

Figure 23. HWTT apparatus.

The criteria for performance are the maximum acceptable rut depth of 12.5 mm and the stripping inflection point from which moisture induced damage is initiated. With their aggregate interlock and sufficient binder content, well designed HMA mixes should perform well in this test. At the same time, the HWTT provides an efficient way to characterize the durability of mixtures subjected to combined loading and moisture conditions which is indispensable for performance-based mixture design and quality control [57].

2.3.3. BBR Evaluation of Asphalt Mixtures

The low temperature performance and deformation resistance of asphalt mixtures were tested using the BBR test in accordance with AASHTO TP 125 [58], and the standard ASTM D8225 [59]. The rectangular beam specimens were obtained directly from laboratory-compacted HMA mixtures and conditioned at low target testing temperatures. In the test, the center point of each simply supported beam specimen was embedded with a load of 980 mN which was maintained for 240 s to monitor linear viscoelastic deflection changes over time to acquire mixture creep stiffness (S) and the rate of creep

(m-value). These parameters were used to assess the resistance of HMA mixtures to low-temperature cracking, with lower stiffness and higher m-values indicating improved cracking resistance. HMA BBR specimens were prepared by cutting small prismatic beams from laboratory-compacted mixture samples produced using a gyratory compactor. The top and bottom portions of each specimen were first removed to obtain a uniform and representative section, followed by a thin cleaning cut. A slice approximately 12.7 mm thick was then cut and trimmed on three sides to form a regular rectangular strip. This strip was subsequently sawn into individual beam specimens with nominal dimensions of 6.35 mm (thickness) × 12.7 mm (width) × 127 mm (length), as shown in Figure 24. The prepared beams were checked for dimensional consistency and conditioned at the test temperature prior to BBR testing.

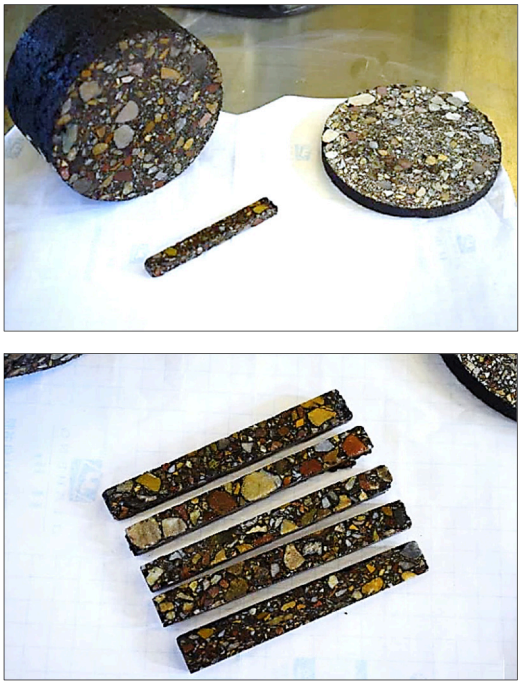

Figure 24. HMA BBR specimens' preparation.

During the BBR test, four beam specimens were prepared for each mix type. Each specimen was simply supported at two ends and subjected to a constant load P applied at midspan, as shown in Figure 25. Upon loading, the midspan deflection $\delta(t)$ was continuously recorded as a function of time over a loading duration of 240 s. The recorded time-dependent deflection response was used to characterize the low-temperature creep behavior of the asphalt mixture.

The creep stiffness, $S(t)$, at a given loading time (t = 60 s) was calculated using classical beam theory as:

$$S(t) = \frac{PL^2}{4bh^3\delta(t)}$$

P = applied constant load (N);
L = span length between supports (mm);
b = beam width (mm);
h = beam thickness (mm);
$\delta(t)$ = midspan deflection at time t (mm).

The creep rate (m-value) represents the ability of the material to relax in terms of stresses and was determined as the slope of the logarithmic stiffness–time relationship using the following equation:

$$m = \left| \frac{d\log S(t)}{d\log t} \right|$$

$d\log S(t)$ = an infinitesimal change in the logarithm of creep stiffness;

$d\log t$ = an infinitesimal change in the logarithm of loading time.

The m-value was obtained from the slope of the logarithmic stiffness–time curve, determined by linear regression of $\log S(t)$ versus $\log t$ around 60 s.

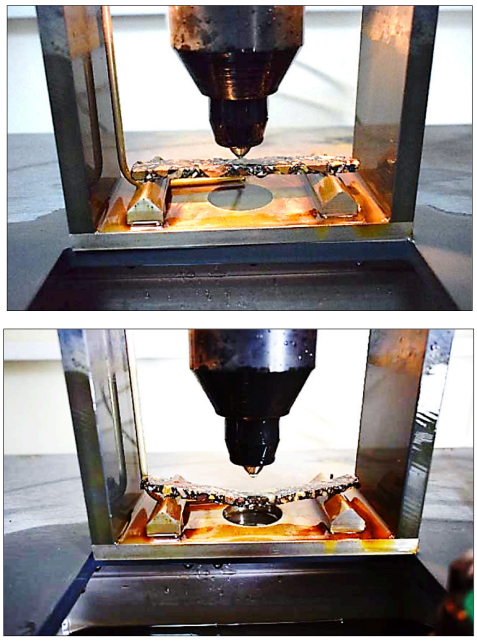

Figure 25. HMA BBR specimens before and after testing.

3. Results and Discussions

3.1. Optimum Rejuvenator Dosages by Weight of Binder Based on PG

3.1.1. In Terms of WEO

WEO exhibited a clear dosage-dependent rejuvenation effect on blended binders with increasing RAP content. At 50% RAP, a WEO dosage of approximately 8% effectively restored the binder from PG 70-16 to PG 64-16, as shown in Figure 26. At 75% RAP, higher WEO dosages of approximately 10% were required to shift the binder from PG 70-10 to PG 64-16 due to the dominance of aged RAP binder, as shown in Figure 27.

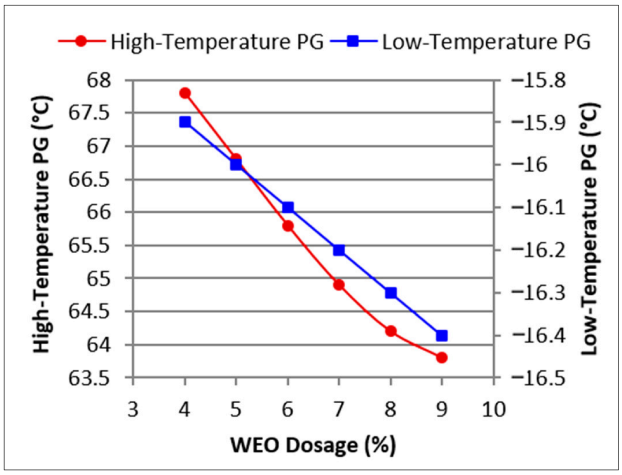

Figure 26. The effect of WEO dosage on PGs of the 50% RAP blend.

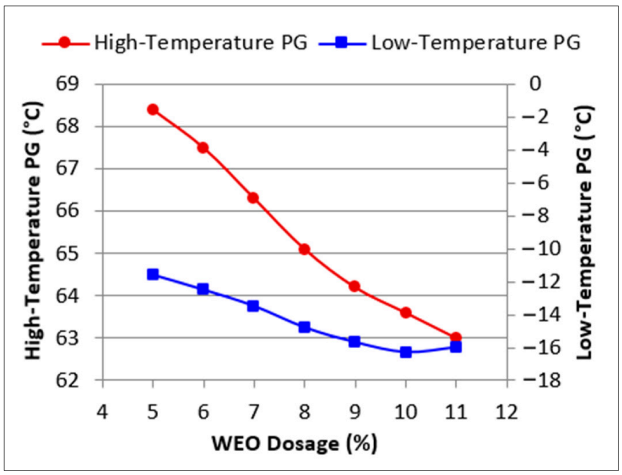

Figure 27. The effect of WEO dosage on PGs of the 75% RAP blend.

3.1.2. In Terms of WCO

WCO exhibited a gradual, RAP-dependent rejuvenation effect. At 50% RAP, approximately 9% WCO was sufficient to adjust the binder from PG 70-16 to the target PG 64-16 while preserving low-temperature performance, as shown in Figure 28. At 75% RAP, higher WCO dosages of about 12% were required to shift the binder from PG 70-10 to PG 64-16 due to the dominance of aged RAP binder, as shown in Figure 29.

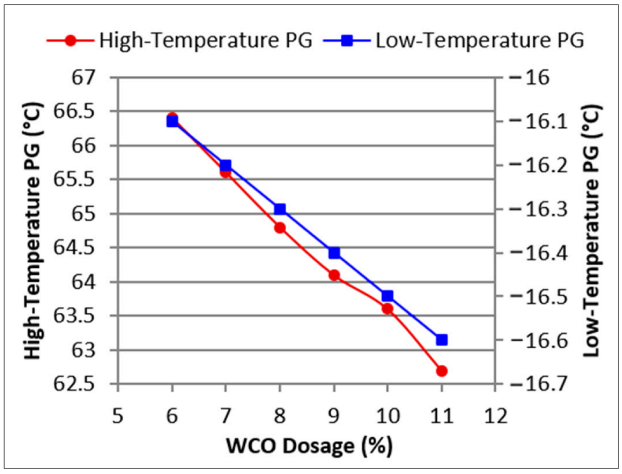

Figure 28. The effect of WCO dosage on PGs of the 50% RAP blend.

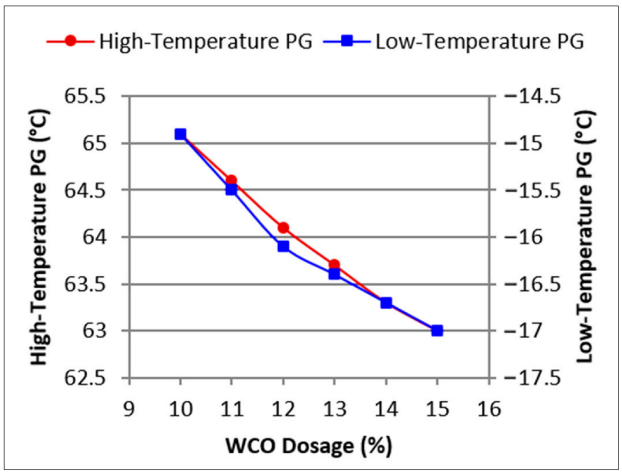

Figure 29. The effect of WCO dosage on PGs of the 75% RAP blend.

3.1.3. In Terms of YG

YG exhibited a RAP-dependent rejuvenation response, with decreasing effectiveness at higher RAP contents. At 50% RAP, approximately 9% YG was sufficient to restore the binder from PG 70-16 to PG 64-16 while maintaining low-temperature performance, as shown in Figure 30. At 75% RAP, the dominance of aged RAP binder required higher YG dosages, with an optimum of about 14% to shift the binder from PG 70-10 to PG 64-16, as shown in Figure 31.

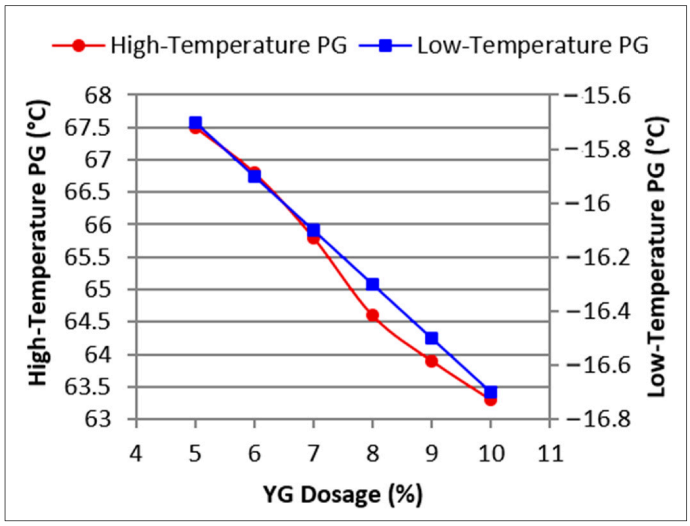

Figure 30. The effect of YG dosage on PGs of the 50% RAP blend.

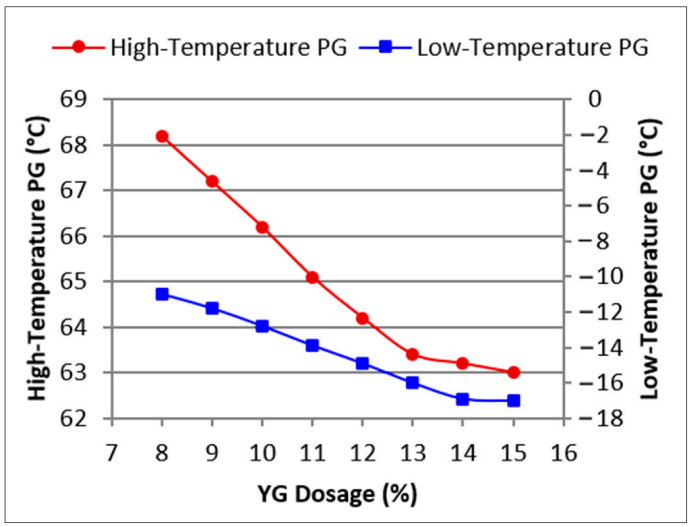

Figure 31. The effect of YG dosage on PGs of the 75% RAP blend.

3.1.4. In Terms of WHO

WHO exhibited a RAP-dependent rejuvenation response. At 50% RAP, approximately 7% WHO effectively restored the binder from PG 70-16 to PG 64-16 while maintaining low-temperature performance, as shown in Figure 32. At 75% RAP, the dominance of aged RAP binder required higher WHO dosages, with an optimum of about 11% to shift the binder from PG 70-10 to PG 64-16, as shown in Figure 33.

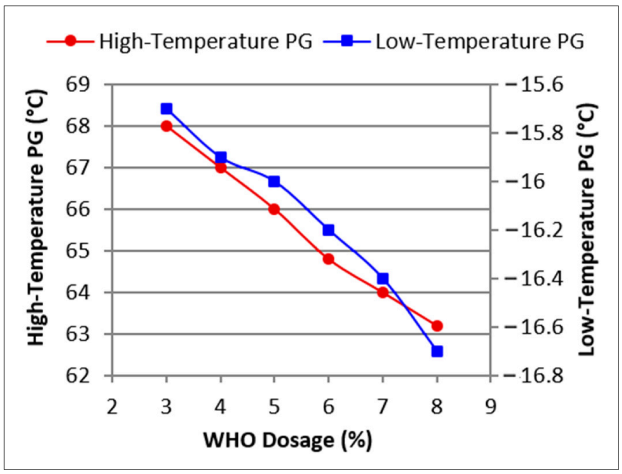

Figure 32. The effect of WHO dosage on PGs of the 50% RAP blend.

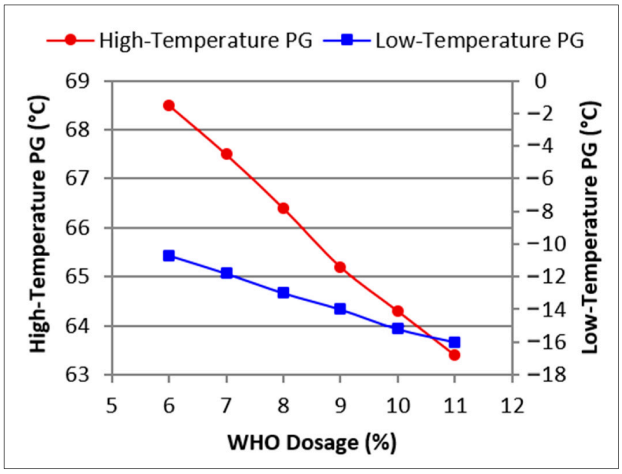

Figure 33. The effect of WHO dosage on PGs of the 75% RAP blend.

3.1.5. In Terms of WETO

WETO exhibited a strong, RAP-dependent rejuvenation effect. At 50% RAP, approximately 6% WETO was sufficient to restore the binder from PG 70-16 to PG 64-16 while maintaining low-temperature performance, as shown in Figure 34. At 75% RAP, the dominance of aged RAP binder required higher WETO dosages, with an optimum of about 10% to shift the binder from PG 70-10 to PG 64-16, as shown in Figure 35.

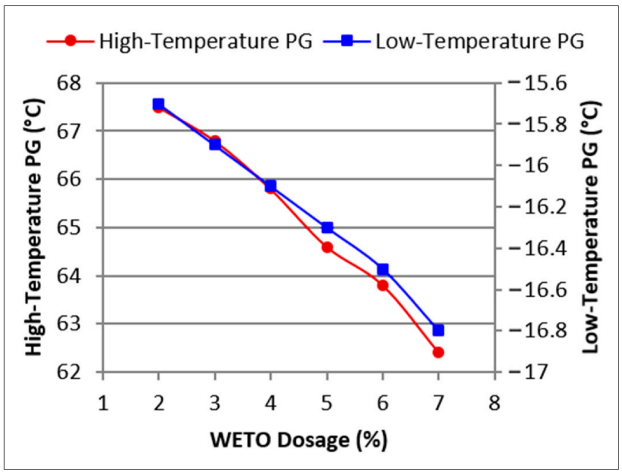

Figure 34. The effect of WETO dosage on PGs of the 50% RAP blend.

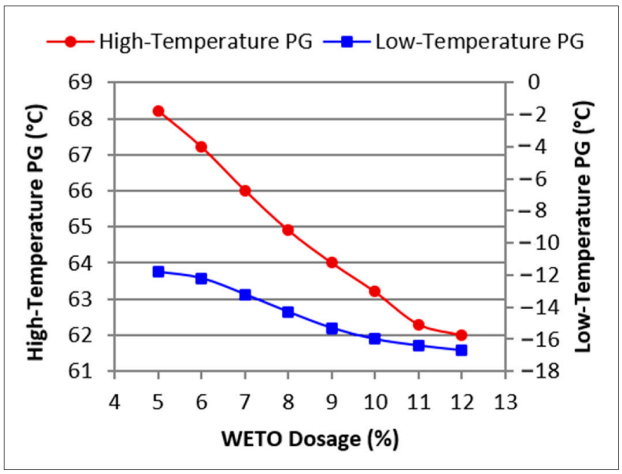

Figure 35. The effect of WETO dosage on PGs of the 75% RAP blend.

3.1.6. In Terms of SO

Slop oil, SO, exhibited a RAP-dependent, moderate rejuvenation response. At 50% RAP, approximately 8% SO was sufficient to restore the binder from PG 70-16 to PG 64-16 while maintaining low-temperature performance, as shown in Figure 36. At 75% RAP, the dominance of aged RAP binder required higher SO dosages, with an optimum of about 13% to shift the binder from PG 70-10 to PG 64-16, as shown in Figure 37.

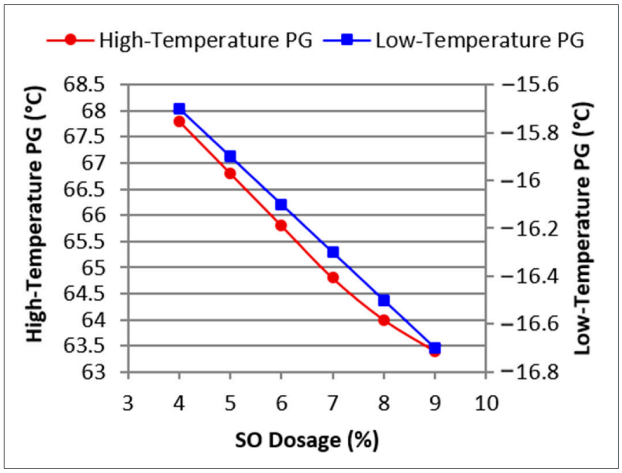

Figure 36. The effect of SO dosage on PGs of the 50% RAP blend.

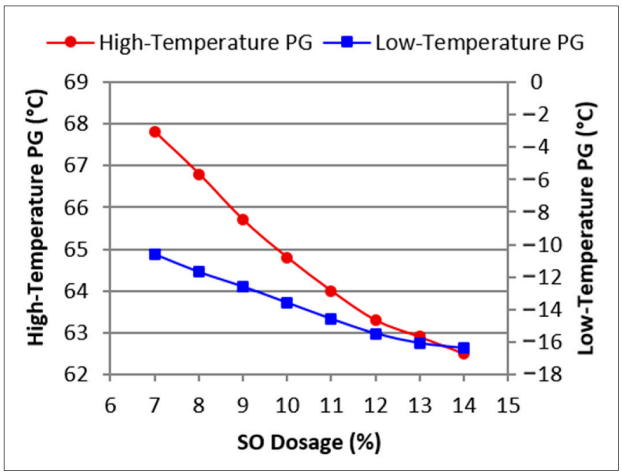

Figure 37. The effect of SO dosage on PGs of the 75% RAP blend.

3.1.7. In Terms of SDBO

SDBO exhibited a mild-to-moderate, RAP-dependent rejuvenation effect. At 50% RAP, an optimum dosage of approximately 13% was required to restore the binder from PG 70-16 to PG 64-16, as shown in Figure 38. At 75% RAP, the increased dominance of aged RAP binder reduced rejuvenation efficiency, necessitating a higher SDBO dosage of about 18% to achieve the same target grade (PG 64-16), as shown in Figure 39.

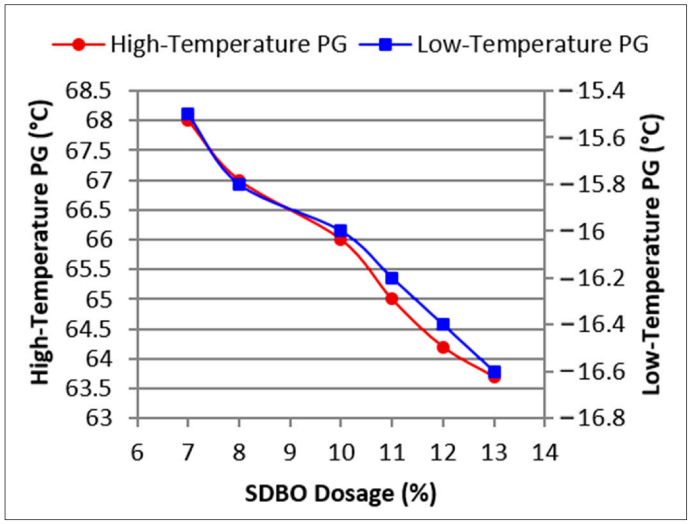

Figure 38. The effect of SDBO dosage on PGs of the 50% RAP blend.

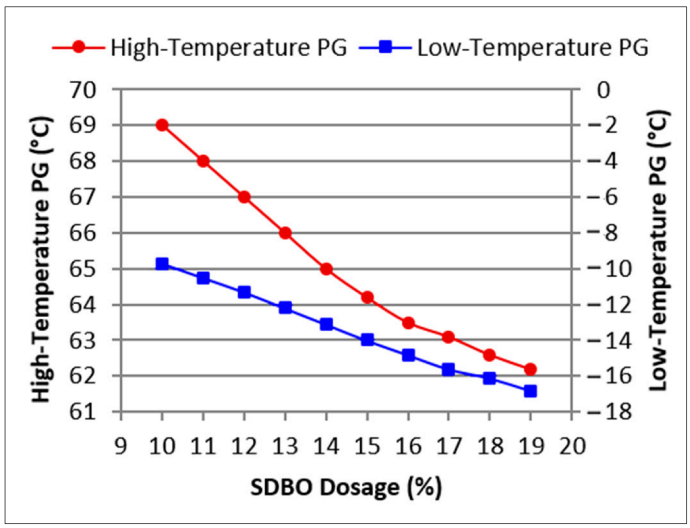

Figure 39. The effect of SDBO dosage on PGs of the 75% RAP blend.

3.1.8. In Terms of TPO

TPO exhibited a RAP-dependent, moderate rejuvenation effect. At 50% RAP, an optimum dosage of approximately 10% restored the binder from PG 70-16 to PG 64-16 while maintaining acceptable low-temperature performance, as shown in Figure 40. At 75% RAP, the dominance of aged RAP binder required higher TPO dosages, with an optimum of about 14% to shift the binder from PG 70-10 toward PG 64-16, as shown in Figure 41.

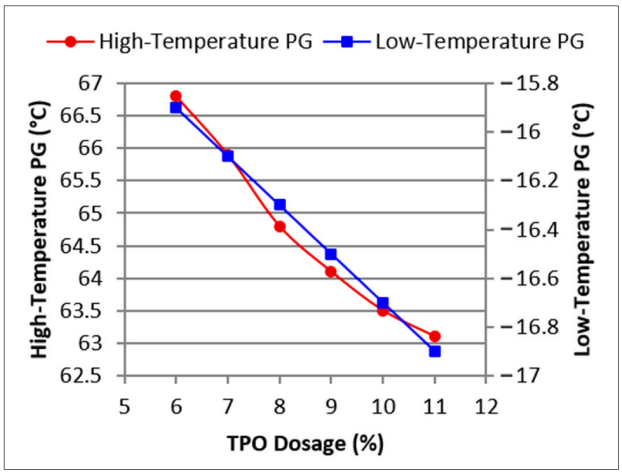

Figure 40. The effect of TPO dosage on PGs of the 50% RAP blend.

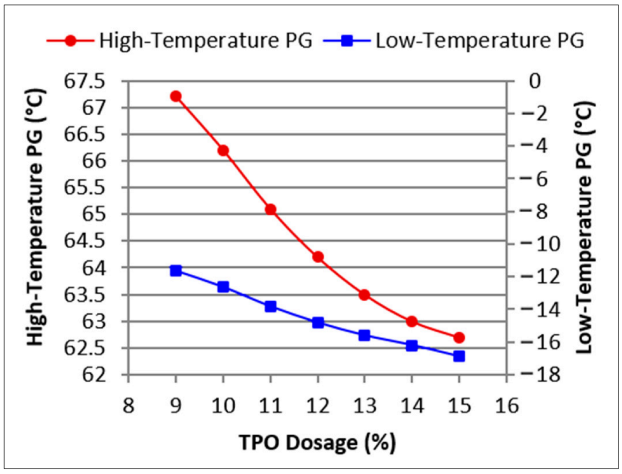

Figure 41. The effect of TPO dosage on PGs of the 75% RAP blend.

3.1.9. In Terms of PPO

PPO exhibited a RAP-dependent, moderate-to-strong rejuvenation effect. At 50% RAP, an optimum dosage of approximately 9% restored the binder from PG 70-16 to PG 64-16 while maintaining low-temperature performance, as shown in Figure 42. At 75% RAP, the increased dominance of aged RAP binder required higher PPO dosages, with an optimum of about 12% to shift the binder from PG 70-10 toward PG 64-16, as shown in Figure 43.

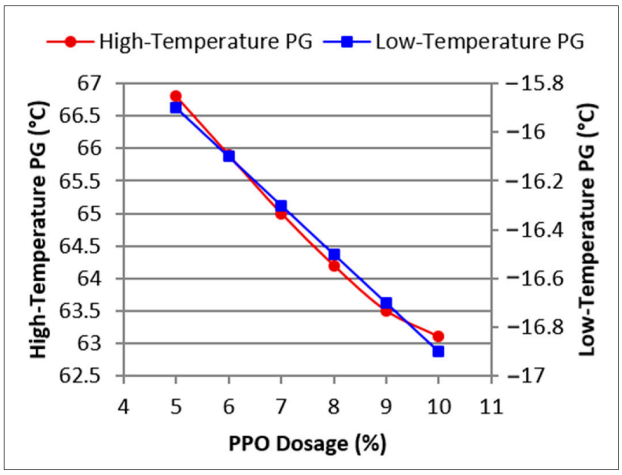

Figure 42. The effect of PPO dosage on PGs of the 50% RAP blend.

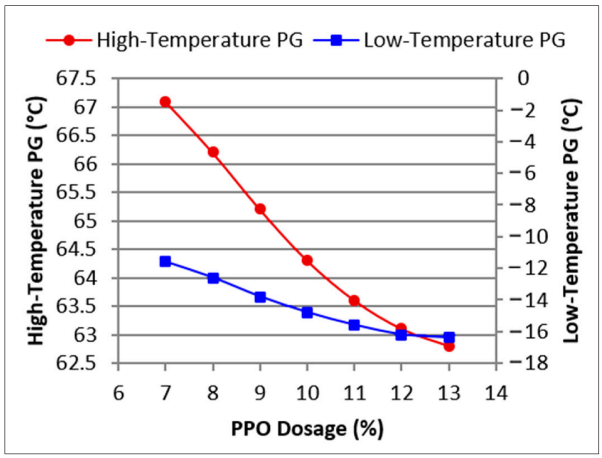

Figure 43. The effect of PPO dosage on PGs of the 75% RAP blend.

3.1.10. In Terms of ARO

ARO exhibited a RAP-dependent, mild rejuvenation effect. At 50% RAP, an optimum dosage of approximately 13% was sufficient to restore the binder from PG 70-16 to PG 64-16 while maintaining acceptable low-temperature performance, as shown in Figure 44. At 75% RAP, the increased dominance of aged RAP binder reduced rejuvenation efficiency, requiring higher ARO dosages, with an optimum of about 18% to shift the binder from PG 70-10 to PG 64-16, as shown in Figure 45.

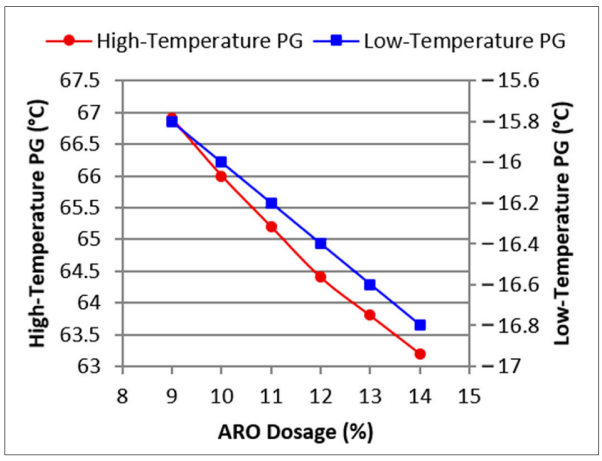

Figure 44. The effect of ARO dosage on PGs of the 50% RAP blend.

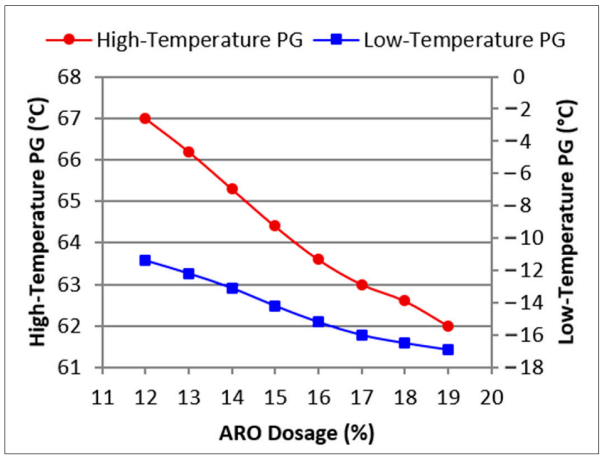

Figure 45. The effect of ARO dosage on PGs of the 75% RAP blend.

Higher RAP content required higher optimum rejuvenator dosages for all evaluated rejuvenators. For both RAP levels, the optimum dosage varied with rejuvenator type, reflecting differences in rejuvenation efficiency, while mixtures with 75% RAP consistently demanded higher dosages than those with 50% RAP due to the increased stiffness and aging severity of the RAP binder, as shown in Figures 46 and 47.

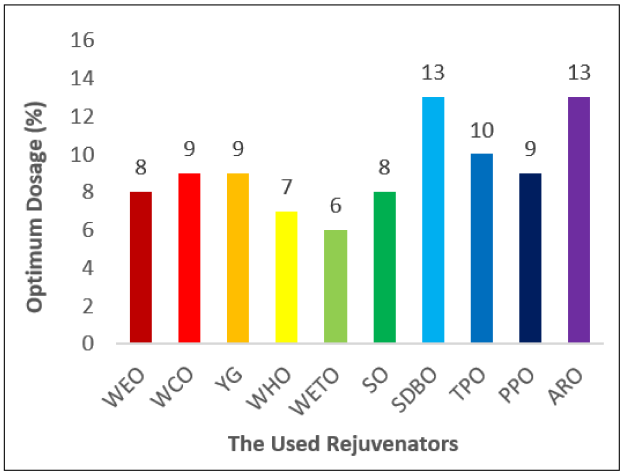

Figure 46. Optimum rejuvenator dosages for recycled HMA mixtures with 50% RAP (PG-based).

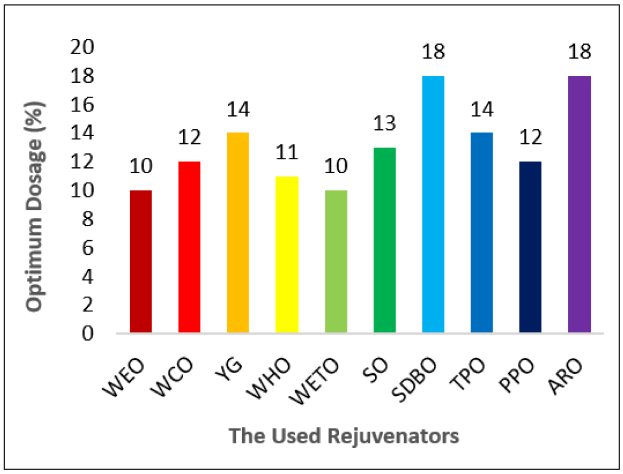

Figure 47. Optimum rejuvenator dosages for recycled HMA mixtures with 75% RAP (PG-based).

3.2. Performance Framework

3.2.1. Superpave Mechanical Properties

The mechanical test performance of the control recycled and rejuvenated HMA mixes contribute valuable information regarding structural response, damage resistance and load carrying characteristics, which are consistent with Superpave acceptance criteria and suggest a suitability for consideration as a durable field mix. The Superpave HMA mixture requirements are presented in Table 22 according to AASHTO M323 [55] specifications.

Table 22. Superpave volumetric criteria (AASHTO M323 [55]).

Property	Specification (AASHTO M323 [55])
Air Voids (Va, %)	3.0–5.0
Voids in Mineral Aggregate (VMA, %) with 12.5 NAMS	≥14.0
Voids Filled with Asphalt (VFA, %)	65–75

Figures 48–50 demonstrate the mechanical behavior of the control, recycled and generated HMA mixtures.

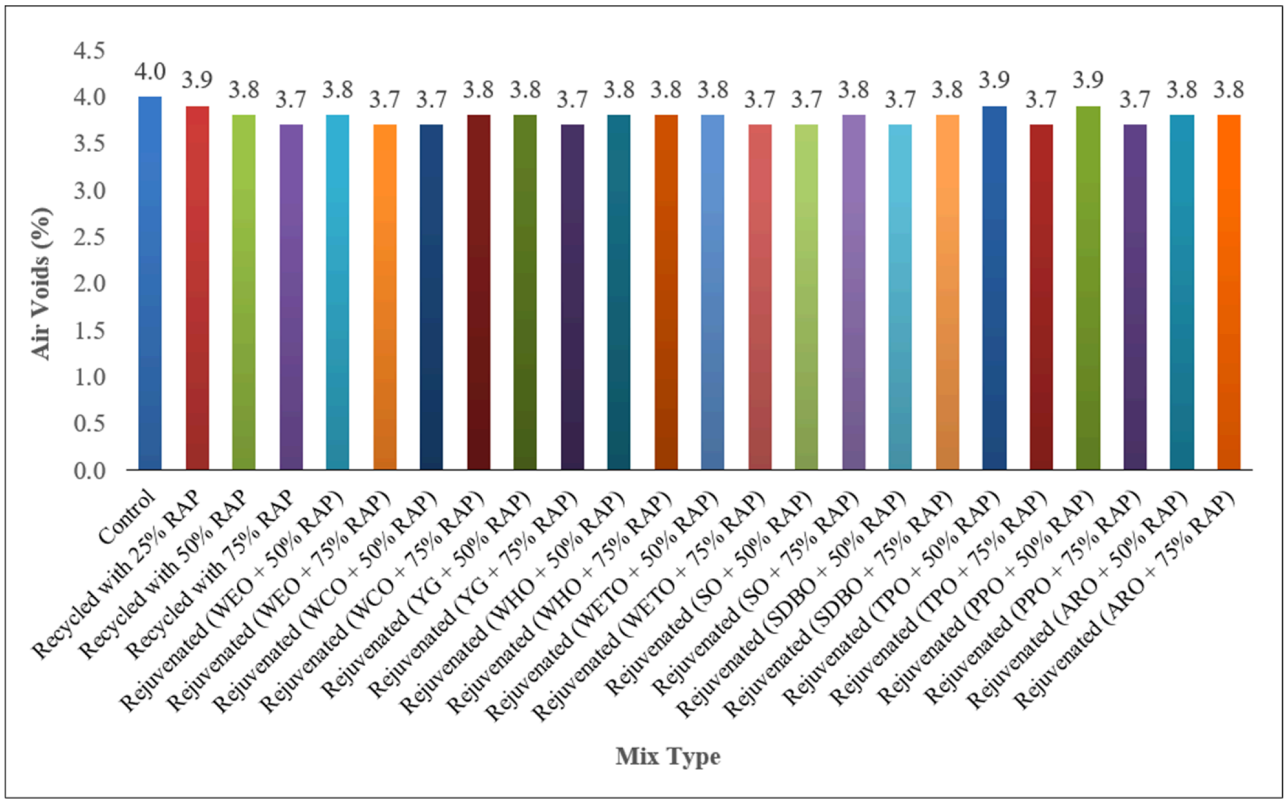

Figure 48. The measured air voids (%) for the control, recycled, and rejuvenated HMA mixtures.

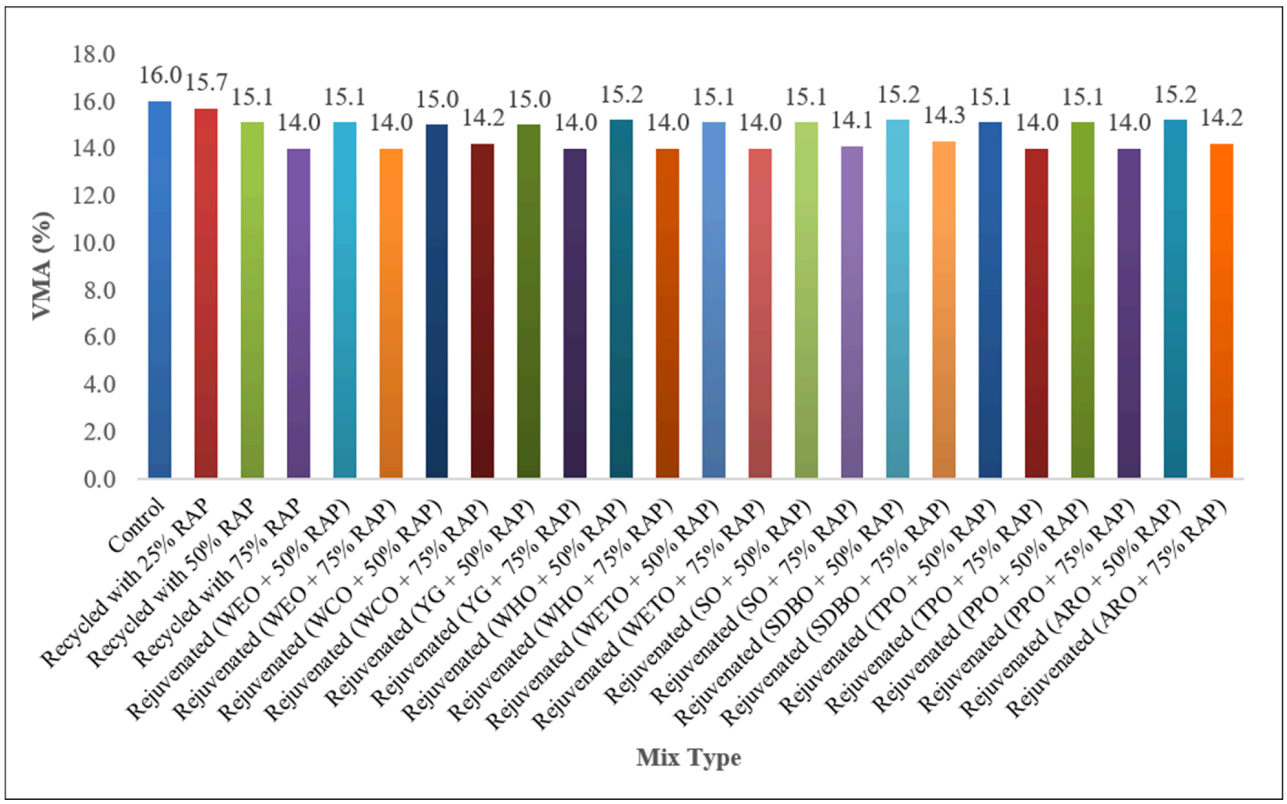

Figure 49. The measured voids in mineral aggregate (%) for the control, recycled, and rejuvenated HMA mixtures.

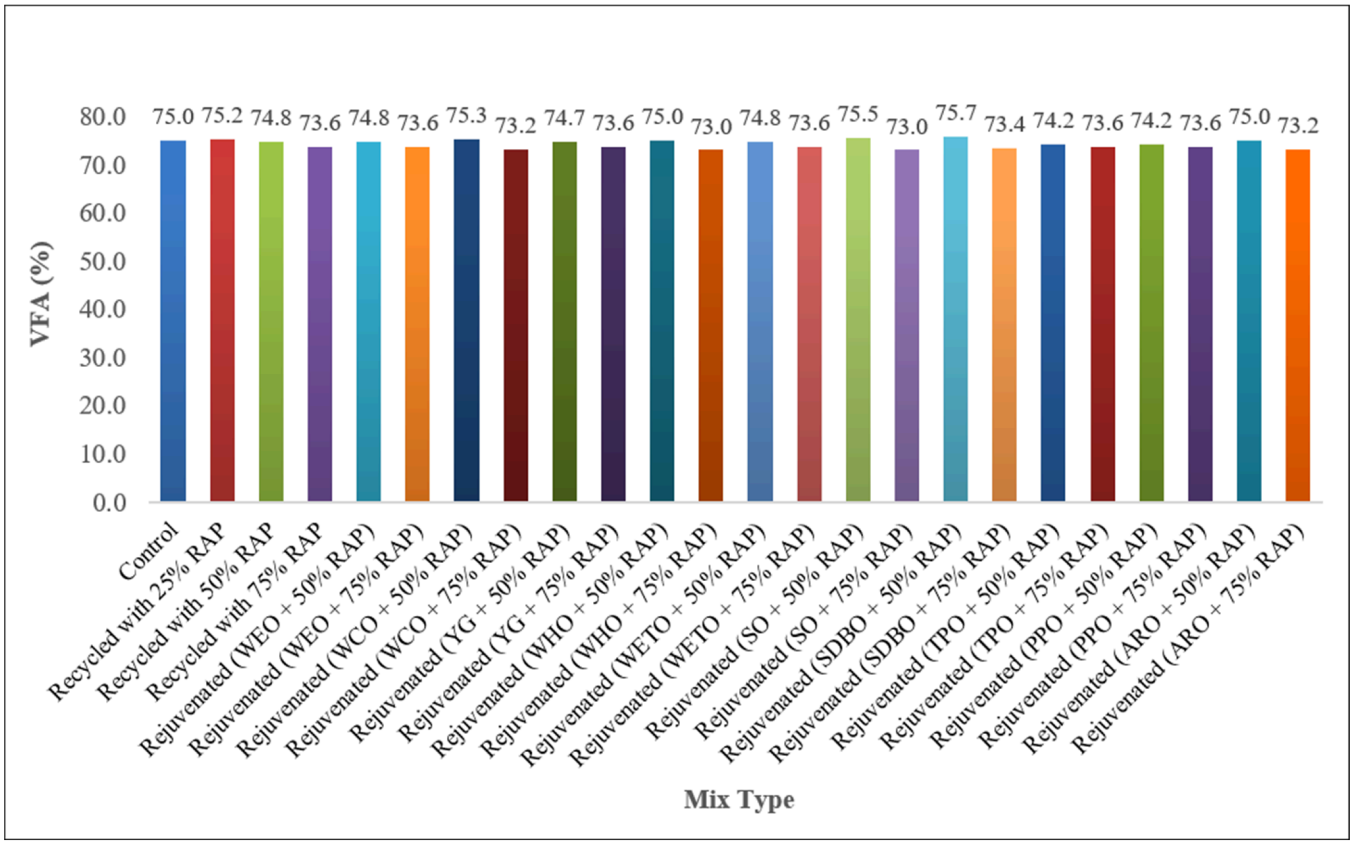

Figure 50. The measured voids filled with asphalt (%) for the control, recycled, and rejuvenated HMA mixtures.

Air voids, VMA and VFA are used to characterize the mechanical equilibrium of the mixtures. Stable air-void contents suggest uniform compaction and controlled densification, while consistent VMA values reveal the aggregate skeleton was not destroyed despite the use of RAP and rejuvenator. The VFA test results also show good binder distribution and void filling in the rejuvenated mixtures, which confirms an improvement of the binder's workability. The softening of the aged RAP binder and increase in mobility during the mixing and compaction process facilitated by rejuvenators can be ascribed to the replenishment of lost maltenes, and a decrease in stiffness (rigidity) with a porous internal structure for RAP mixes. Recycled mixtures had 5–10 and 6–12% lower air voids and VMA because of the stiff aged binder, and comparable (±2–3%) VFA respectively when compared with control mixture at all contents showing acceptable volumetric balance without shortage of the binder. However, rejuvenated mixes exhibited an increased amount of air voids (3–7%) and VMA (5–10%) compared to those not-rejuvenated recycled mixtures, and a slight decrease in VFA of 2–5%, which proved the better binder influence on the mixture mobility and mechanical properties. The results of this study are in agreement with Khan [60], who indicated that the reduction ratio scale value for air voids was 5–8% and VMA was 6–10% for RAP mixtures containing bound oil, as compared to traditional blends because of better binder flexibility and squeezing densification. The results of VFA from his work are within the acceptable VFA range, showing binder re-distribution does not result in a lack of binders. Expanding upon these quantified trends, the current study expands upon this work by further investigating higher RAP contents and comparing multiple rejuvenator types and dosages in a systematic manner, progressing findings of the literature towards a more holistic understanding for high-RAP mix designs.

3.2.2. Wheel-Tracking Test Results (HWTT)

The wheel-tracking results are shown here for rutting resistance assessment of the control, recycled and rejuvenated mixes under repeated wheel pass. This test contributes to the understanding of the interactive influences between RAP content and rejuvenator type on permanent deformation behavior and moisture stability for mixtures. The rut depths of the control, recycled, and rejuvenated mixes at four levels of wheel passes are given in Table 23.

Table 23. Rut depth results at different wheel-passing levels.

Mixture Type	Rut Depth (mm)			
	at 5000 Passes	at 10,000 Passes	at 15,000 Passes	at 20,000 Passes
Control	0.85	1.55	2.28	2.90
Recycled with 25% RAP	0.80	1.45	2.15	2.75
Recycled with 50% RAP	0.65	1.15	1.60	2.00
Recycled with 75% RAP	0.55	0.95	1.30	1.65
Rejuvenated (WEO + 50% RAP)	0.80	1.45	2.05	2.60
Rejuvenated (WEO + 75% RAP)	0.60	1.05	1.45	1.80
Rejuvenated (WCO + 50% RAP)	0.88	1.60	2.25	2.85
Rejuvenated (WCO + 75% RAP)	0.75	1.30	1.85	2.30
Rejuvenated (YG + 50% RAP)	0.90	1.62	2.28	2.88
Rejuvenated (YG + 75% RAP)	0.80	1.55	2.15	2.70
Rejuvenated (WHO + 50% RAP)	0.75	1.35	1.90	2.40
Rejuvenated (WHO + 75% RAP)	0.68	1.18	1.65	2.05
Rejuvenated (WETO + 50% RAP)	0.70	1.25	1.75	2.20
Rejuvenated (WETO + 75% RAP)	0.62	1.08	1.50	1.85
Rejuvenated (SO + 50% RAP)	0.85	1.48	2.10	2.65
Rejuvenated (SO + 75% RAP)	0.80	1.30	2.00	2.50
Rejuvenated (SDBO + 50% RAP)	1.08	1.95	2.70	3.35
Rejuvenated (SDBO + 75% RAP)	1.05	1.85	2.65	3.10
Rejuvenated (TPO + 50% RAP)	0.98	1.75	2.45	3.05

Table 23. *Cont.*

Mixture Type	Rut Depth (mm)			
	at 5000 Passes	at 10,000 Passes	at 15,000 Passes	at 20,000 Passes
Rejuvenated (TPO + 75% RAP)	0.92	1.60	2.25	2.80
Rejuvenated (PPO + 50% RAP)	0.92	1.65	2.32	2.92
Rejuvenated (PPO + 75% RAP)	0.78	1.35	1.90	2.35
Rejuvenated (ARO + 50% RAP)	1.10	1.98	2.75	3.40
Rejuvenated (ARO + 75% RAP)	1.08	1.90	2.70	3.25

Compared to the control mixes, the rut depth of the recycled mixes decreased with increasing RAP content. At 25% RAP rut depth at 20,000 passes was reduced by around 5%, suggesting a slight stiffening. The reduction was increased to approximately 31% at 50% RAP, and almost to 43% at a level of 75% RAP. This tendency is due to the growing contribution of the hard aged RAP binder which greatly increases the resistance against permanent deformations.

At 50 % RAP, the rejuvenated mixes exhibited a controlled rut depth increase compared to the unrejuvenated recycled mix. Rut depth at 20,000 passes was increased by about 10–68%, depending on the type of rejuvenator, due to the softening of the aged binder and restoration of mixture flexibility. Although in certain increases the rut depths are more than comparable to the control mix or slightly higher, an effective trade-off between resistance to rutting and rejuvenation of the binder was retained.

The rut depth of rap mixtures with 75% RAP was about 9 to 88% higher than that of the unrejuvenated recycled mixture when aged (with rejuvenators). This rise is due to the higher amount of rejuvenator that was necessary in order to mitigate significant binder aging. However, when compared with the unaged mixtures, the rejuvenated mixtures still presented satisfactory rutting performances in this regard and showed some rejuvenators that produced rut depths even lower than those obtained with the control mixture, indicating that rejuvenation alleviated excessive stiffness but did not negatively affect resistance to deformation. Higher RAP contents caused rut depth to decrease considerably; however, rejuvenation increased the levels of rutting deliberately in order to recover the mixture flexibility resulting in controlled and performance-complementary behavior at 50% and 75% RAP.

According to the HWTT, the WETO yielded the best results at 50% RAP and the WEO gave the best performance at 75% RAP with lowest rut depth among rejuvenated mixes. The HWTT patterns computed in this study are also consistent with findings from Rafiq et al. [61], who showed recycled HMA mixes had on average 20–40% less rut depth than control mixes due to the stiffening effect of aged RAP binder. They also found the addition of modifiers resulted in a moderate increase in rut depth (approximately 10–30%) when compared with unrejuvenated recycled mixtures, but still acceptable stripping resistance and resistance to rutting. Likewise, the current investigation validates such behavior and expands on the previous works by broadening the scope of study to higher RAP percentages as well as different rejuvenator types, showing that the rut depth increase due to rejuvenation is consistently controlled and performance-bounded for optimal dosage levels.

3.2.3. BBR Results of the Developed HMA Mixtures

The performance of the developed HMA mixtures (control, recycled and rejuvenated) at low temperature is evaluated using BBR results. Attention has been paid to the creep stiffness and creep rate, illustrated above in Figures 51 and 52, that describe the joint mixture's resistance to low-temperature cracking by measuring its strength and stress relaxation performance.

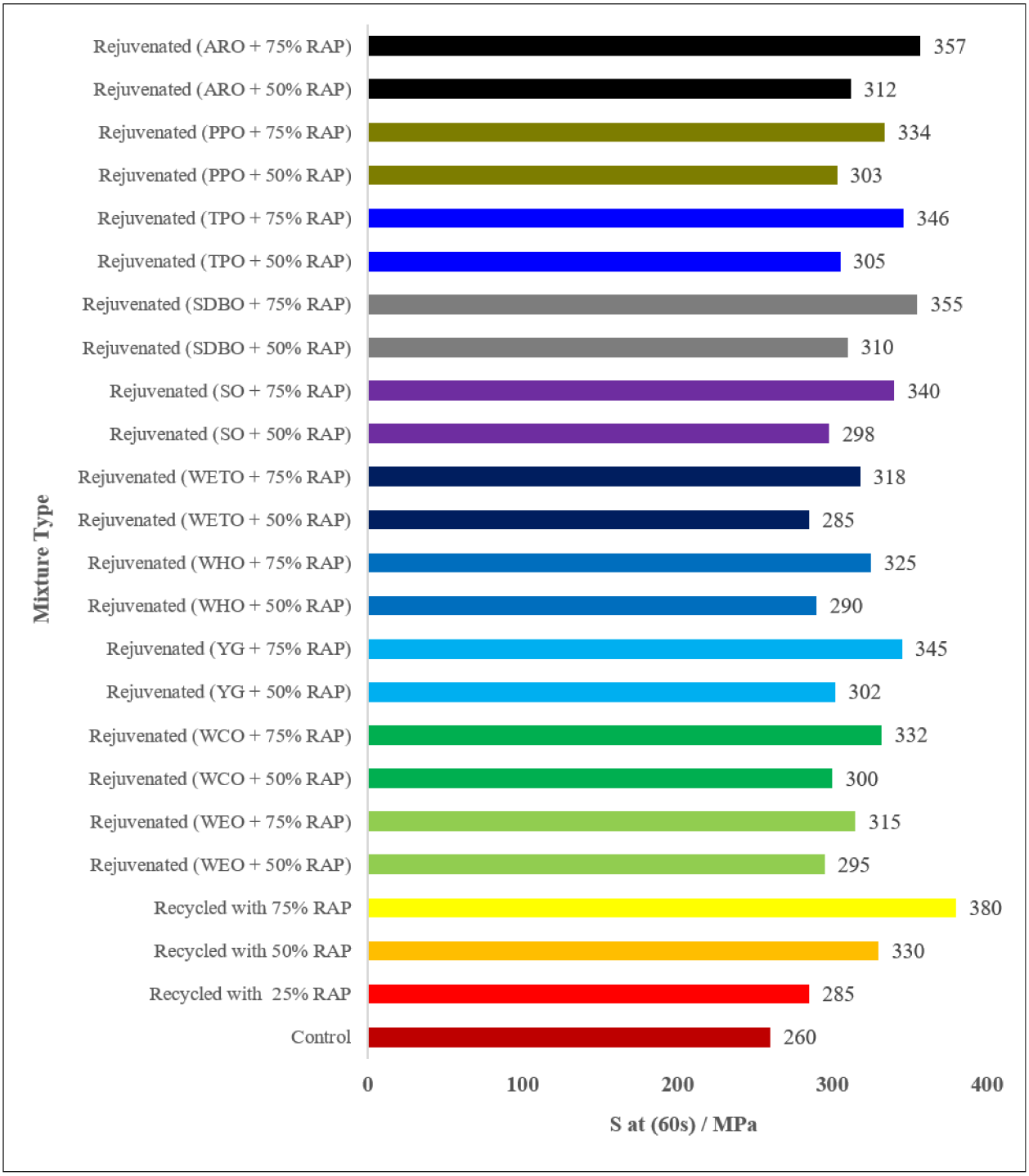

Figure 51. The creep stiffness for the developed HMA mixtures.

The recycled mix exhibited substantially worse low-temperature performance for 50% RAP than the control mixture, with creep stiffness increasing by about 25–30% and

a decline in the creep rate of approximately 10–15%, observing higher brittleness and cracking potential. The introduction of rejuvenator is the turning factor to this rule: the stiffness decreases approximately by 10–15% and creep rate increases about by 7–10%, compared with those of unrejuvenated recycled mixture, showing an improvement in flexibility and stress relaxation property.

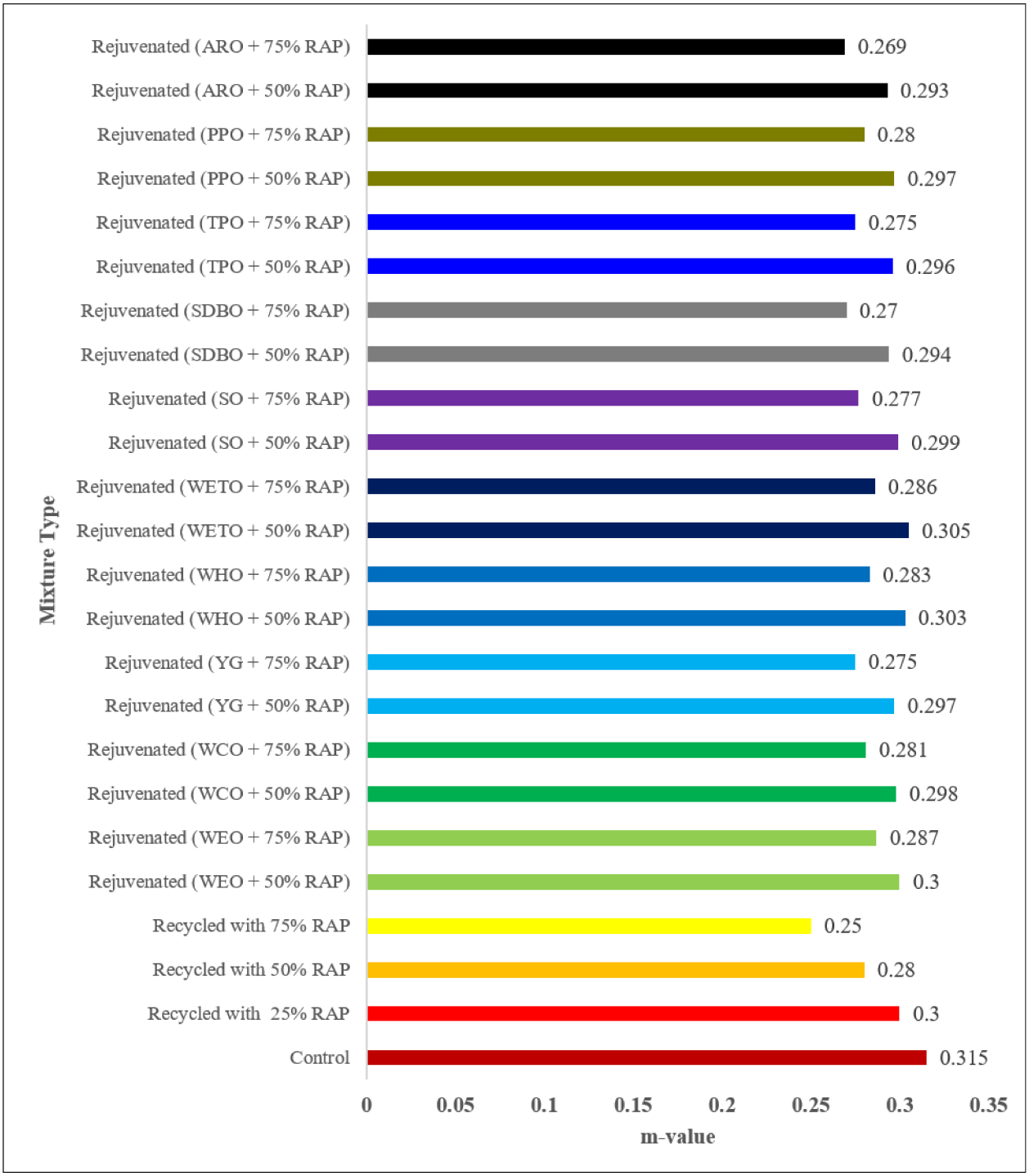

Figure 52. The creep rate for the developed HMA mixtures.

At 75% RAP, the aging effect is exasperated where the creep stiffness increases by approximately 45–50%, and the rate of creep decreases by around 20–25%, when compared to the control which results in poor LT cracking resistance. Rejuvenated mixtures at this RAP level show a 12–18% decrease in stiffness and about 10–15% higher creep rate

than those of the unrejuvenated recycled mixture, demonstrating a partial but significant improvement of low-temperature cracking resistance.

Increased creep stiffness together with decreased creep rate results in lower stress relaxation and a greater risk of thermal cracking, while reduced stiffness and higher creep rate indicate improved low-temperature behavior. Among the rejuvenators considered, WETO gives the highest effectiveness at 50% RAP and WEO and WETO give the highest performances at 75% RAP, where they both yield the greatest reduction in stiffnesses and improvement in creep rates.

The results of the current study are consistent with Saed et al. [62]; the recycling agents at the binder reduced stiffness about 10–25% and increased creep rate by 8–20%, but aging had an opposite trend. The findings indicate an increase in RAP content causes the creep stiffness to increase and the creep rate to decrease, while rejuvenation causes the opposite. Compared to previous binder-level analyses, the novelty of this work is assessing mixture performance across multiple rejuvenators at high RAP contents, which better represents a practical approach for the design of durable high-RAP mixtures.

3.3. Statistical Analysis

3.3.1. Correlation and Linear Regression Analysis

The analyses of correlation and linear regression were conducted to examine the relationship between rejuvenator dosage and the measured performance tests for the developed recycled mixtures in terms of rutting resistance. Two types of recycled mixtures were presented in accordance with RAP content.

- Recycled mixture with 50% RAP

The values of rutting depths for the recycled mixtures prepared with the optimum rejuvenator dosages were extracted for the experimental part above, Figure 46 and Table 23, and summarized in Table 24, below.

Table 24. The data used for the correlation and regression analyses of 50% RAP mixtures.

Rejuvenator Type	Optimum Dosage, D (%)	Rut Depth, RD (mm)
WETO	6	2.20
WHO	7	2.40
WEO	8	2.60
SO	8	2.65
WCO	9	2.85
YG	9	2.88
PPO	9	2.92
TOP	10	3.05
SDBO	13	3.35
ARO	13	3.40

D = Optimum dosage of rejuvenator (%); RD = Rut depth at 20,000 passes (mm).

1. Regression Analysis

The model of regression is

$$RD = aD + b$$

where:

a = Slope;

b = Intercept;

$$a = \frac{n\sum D \times RD - (\sum D) \times (\sum RD)}{n\sum D^2 - (\sum D)^2}$$

n = The number of observations (equals to 10 in our case);
$\sum D = 92$;
$\sum RD = 28.30$;
$\sum D^2 = 894$;
$\sum D \times RD = 268.10$.

$$a = \frac{10 \times (268.10) - 92 \times (28.30)}{10 \times 894 - 92^2} = 0.1626$$

$$b = \frac{\sum RD - a \times \sum D}{n}$$

$$b = \frac{28.30 - (0.1626) \times (92)}{10} = 1.3341$$

$$RD = 0.1626D + 1.3341$$

2. Correlation Analysis

$$Pearson\ correlation\ coefficient\ (r) = \frac{n\sum D \times RD - (\sum D) \times (\sum RD)}{\sqrt{\left[n\sum D^2 - (\sum D)^2\right] \times \left[n\sum RD^2 - (\sum RD)^2\right]}}$$

$$r = \frac{77.4}{\sqrt{476 \times 13.341}} = 0.972$$

This indicates a very strong correlation.

3. Coefficient of Determination

$$R^2 = r^2$$

$$R^2 = (0.972)^2$$

$$R^2 = 0.945$$

The achieved results in terms of correlation and regression analysis for the 50% RAP are shown below in Figure 53.

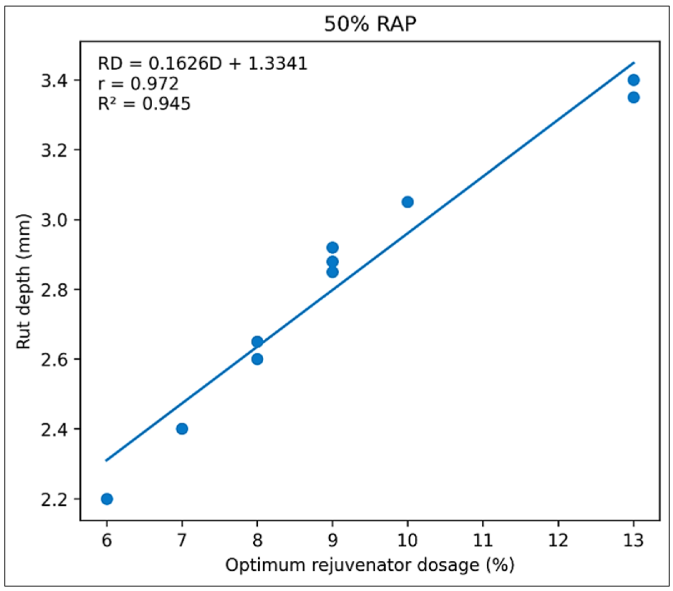

Figure 53. Correlation and linear regression analysis for 50% RAP mixtures.

Recycled mixture with 75% RAP

The values of rutting depths for the recycled mixtures prepared with the optimum rejuvenator dosages were extracted for the experimental part above, Figure 47 and Table 23, and summarized in Table 25, below.

Table 25. The data used for the correlation and regression analyses of 75% RAP mixtures.

Rejuvenator Type	Optimum Dosage, D (%)	Rut Depth, RD (mm)
WETO	10	1.80
WHO	10	1.85
WEO	11	2.05
SO	12	2.30
WCO	12	2.35
YG	13	2.50
PPO	14	2.70
TOP	14	2.80
SDBO	18	3.10
ARO	18	3.25

1. Regression Analysis

$\sum D = 132$;
$\sum RD = 24.70$;
$\sum D^2 = 1818$;
$\sum D \times RD = 338.65$.

$$a = \frac{10 \times (338.65) - 132 \times (24.70)}{10 \times 1818 - 132^2} = 0.1668$$

$$b = \frac{24.70 - (0.1668) \times (132)}{10} = 0.2682$$

$$RD = 0.1668D + 0.2682$$

2. Correlation Analysis

$$r = \frac{126.1}{\sqrt{756 \times 21.91}} = 0.979$$

This indicates a very strong correlation.

3. Coefficient of Determination

$$R^2 = r^2$$

$$R^2 = (0.979)^2$$

$$R^2 = 0.958$$

The achieved results in terms of correlation and regression analysis for the 75% RAP are shown below in Figure 54.

The correlation and regression analyses revealed a strong relationship between rejuvenator dosage and rut depth for both 50% RAP (r = 0.972, R^2 = 0.945) and 75% RAP (r = 0.979, R^2 = 0.958) mixtures, indicating that lower rejuvenator dosages generally resulted in better rutting resistance.

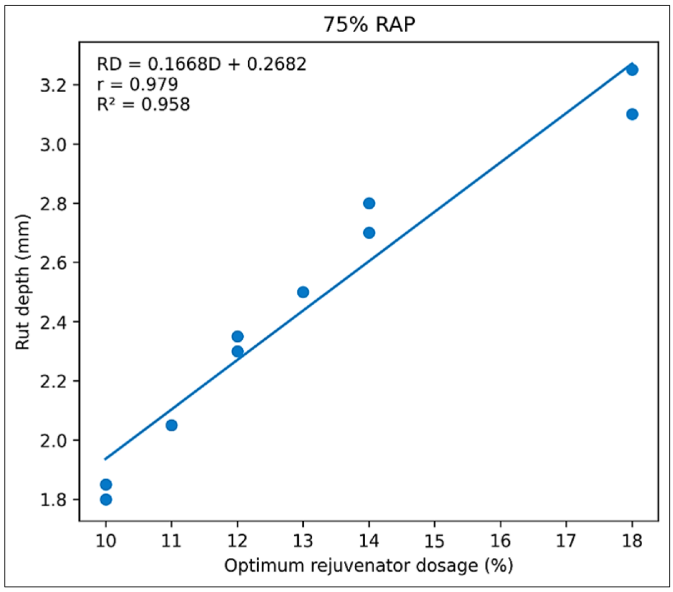

Figure 54. Correlation and linear regression analysis for 75% RAP mixtures.

3.3.2. Performance Index (PI) Analysis

A PI was developed based on HWTT rut depth, BBR stiffness, and BBR m-value to provide a quantitative comparison among the employed rejuvenators. The experimental data were adopted from Table 23, and Figures 51 and 52, and summarized in Table 26 below.

Table 26. The experimental results used in the PI analysis.

Rejuvenator Type	50% RAP-Recycled Mixture			75% RAP-Recycled Mixture		
	Rut Depth (mm), RD	S (MPa), S	m-Value, m	Rut Depth (mm), RD	S (MPa), S	m-Value, m
WEO	2.60	295	0.300	1.80	315	0.287
WCO	2.85	300	0.298	2.30	332	0.281
YG	2.88	302	0.297	2.70	345	0.275
WHO	2.40	290	0.303	2.05	325	0.283
WETO	2.20	285	0.305	1.85	318	0.286
SO	2.65	298	0.299	2.50	340	0.277
SDBO	3.35	310	0.294	3.10	355	0.27
TPO	3.05	305	0.296	2.80	346	0.275
PPO	2.92	303	0.297	2.35	334	0.280
ARO	3.40	312	0.293	3.25	357	0.269

The performance index (PI) is conducted as follows:

$$PI = \frac{RD_n + S_n + m_n}{3}$$

where:

RD_n = Normalized indicator of rutting resistance;
S_n = Normalized indicator of creep stiffness;
m_n = Normalized indicator of creep rate.

Therefore, PI values were calculated depending on date, extracted from Table 26 above and summarized in Table 27, below.

The PI analysis confirmed the trends observed in the performance tests. WETO achieved the highest PI value at 50% RAP, while WEO ranked first at 75% RAP, indicating the best overall balance between rutting resistance and low-temperature performance. Overall, the PI rankings were in good agreement with the experimental results.

Table 27. The PI results of the investigated rejuvenators.

Rejuvenator Type	Performance Index (PI)	
	50% RAP-Recycled Mixture	75% RAP-Recycled Mixture
WETO	1.000	0.946
WHO	0.827	0.789
WEO	0.627	1.000
SO	0.548	0.455
WCO	0.440	0.639
YG	0.379	0.333
PPO	0.356	0.593
TPO	0.267	0.302
SDBO	0.066	0.069
ARO	0.000	0.000

4. Conclusions

This study presents a comprehensive comparative evaluation of waste oils used as rejuvenators in recycled hot mix asphalt mixtures containing different RAP contents. By integrating Superpave mechanical properties, wheel-tracking performance, and BBR-based creep stiffness and creep rate, the conclusions highlight the effectiveness of waste oil rejuvenation in restoring performance, improving durability, and supporting the sustainable use of high-RAP asphalt mixtures. The experimental results were further examined using correlation, regression, and PI analyses. In addition, the investigated waste oils demonstrated promising potential for practical and industrial applications due to their availability and compatibility with conventional asphalt production procedures. The following conclusions highlight the main findings of this study.

1. Based on performance grade evaluation, WETO at 50% RAP (6%) and WEO at 75% RAP (10%) were the most effective rejuvenators, as they enhanced the blended binder and restored its properties to perfectly match the original virgin binder grade PG 64-16 at relatively low dosages.
2. Based on the Superpave mechanical properties evaluation, all the rejuvenated mixtures satisfied the air void, VMA, and VFA requirements and exhibited volumetric properties comparable to those of the control mixture, demonstrating the effectiveness of waste oil rejuvenators in restoring mixture balance and compaction quality. The minimal differences among the rejuvenators indicate a consistently stable mechanical response, confirming that performance-based tests are the key criteria for distinguishing rejuvenator efficiency in high-RAP HMA mixtures.
3. Based on the HWTT results, WETO exhibited the most favorable performance at 50% RAP, while WEO exhibited similar performance at 75% RAP, as evidenced by the lowest rut depths among the rejuvenated mixtures under repeated loading, specifically 20,000 passes.
4. Based on the BBR evaluation of rejuvenated recycled HMA mixtures, WETO is the most effective rejuvenator at 50% RAP, while WEO and WETO provide the best performance at 75% RAP, achieving the greatest reductions in creep stiffness and the most pronounced improvements in creep rate among the evaluated rejuvenators.
5. The statistical analyses supported the experimental findings, revealing strong relationships between rejuvenator dosage and rutting performance for both RAP contents. The PI analysis further identified WETO and WEO as the most effective rejuvenators for the 50% and 75% RAP mixtures, respectively, providing the best overall balance between rutting resistance and low-temperature performance.

The study conclusions indicate that mixture performance generally corresponded to the binder regeneration results. WETO, WHO, WEO, SO, PPO, WCO, and YG recovered

the target binder grade (PG 64-16) at relatively lower dosages and generally showed better overall mixture performance. Among the used waste oils, WETO at 50% RAP and WEO at 75% RAP showed the most significant behavior, as reflected by the lowest rut depths and the improved response of BBR. TPO showed moderate effectiveness, whereas SDBO and ARO required the highest dosages to achieve the target binder grade. Overall, the mixtures tended to perform better when the corresponding waste oil was more effective in restoring the properties of the aged binder.

This study is limited to laboratory-based performance tests, and the results may not fully represent long-term field behavior under varying traffic and environmental conditions. In addition, performance was evaluated using a selected set of tests, while other critical aspects such as long-term aging, and moisture damage evolution, were not addressed. Moreover, the findings are also limited to the investigated materials, virgin binder, and RAP source used in this study.

Furthermore, the chemical characterization of the used waste oils was not addressed in this study, limiting a deeper interpretation of the observed differences in rejuvenation performance. Future work should incorporate extended aging, in-service performance monitoring, and chemical characterization techniques in terms of Fourier Transform Infrared Spectroscopy (FTIR), Saturates-Aromatics-Resins-Asphaltenes (SARA) analysis, Gas Chromatography–Mass Spectrometry (GC-MS), and elemental analysis to provide a deeper understanding of binder regeneration mechanisms and validate the long-term effectiveness of the rejuvenated mixtures.

Author Contributions: Conceptualization, B.S.M.; Methodology, S.A.S. and N.S.K.; Formal analysis, T.M.H.; Investigation, T.M.H.; Writing—original draft, B.S.M., S.A.S. and N.S.K.; Writing—review & editing, B.S.M., S.A.S., N.S.K., Z.A.-K. and T.M.H.; Supervision, M.S.N. and A.S.; Project administration, M.S.N. and A.S. All authors have read and agreed to the published version of the manuscript.

Funding: This research received no external funding.

Data Availability Statement: The data supporting the findings of this study are available from the corresponding author upon reasonable request.

Conflicts of Interest: The authors declare no conflicts of interest.

References

1. Razali, R.; Hainin, M.R.; Hassan, N.A.; Satar, M.K.I.M.; Abdulrahman, S.; Kamarudin, S.N.N. Sustainable asphalt innovation: Harnessing treated waste cooking oil for enhanced warm mix rubberized pavement. *Innov. Infrastruct. Solut.* **2025**, *10*, 445. [CrossRef]
2. Shahsamandy, A.S.; Alae, M.; Xiao, F. Harnessing waste materials for aged asphalt binder revitalization through investigation of rejuvenation mechanism and performance enhancement. *J. Clean. Prod.* **2025**, *493*, 144972. [CrossRef]
3. Hashim, T.M.; Nasr, M.S.; Jebur, Y.M.; Kadhim, A.; Alkhafaji, Z.; Baig, M.G.; Adekunle, S.K.; Al-Osta, M.A.; Ahmad, S.; Yaseen, Z.M. Evaluating Rutting Resistance of Rejuvenated Recycled Hot-Mix Asphalt Mixtures Using Different Types of Recycling Agents. *Materials* **2022**, *15*, 8769. [CrossRef] [PubMed]
4. Wu, H.; Gong, L.M.; Guo, L.; Zhang, L.Y.; Li, J.T. Effects of the free fatty acid content in yellow grease on performance, carcass characteristics, and serum lipids in broilers. *Poult. Sci.* **2011**, *90*, 1992–1998. [CrossRef] [PubMed]
5. Duque-Sarmiento, D.A.; Baño-Morales, D.A. Assessment of Hydraulic Oil Properties during Operation of a Mini Loader. *Lubricants* **2024**, *12*, 320. [CrossRef]
6. Surendranath, M.; Sivakumar, M. Effect of Waste Transformer Oil (WTO) and Waste Engine Oil (WEO) on the Performance of 100% RAP Mixes at Reduced Mixing Temperatures. In *Lecture Notes in Civil Engineering*; Springer: Singapore, 2025; pp. 93–106. [CrossRef]
7. Okon, K.P.; Inyang, E.O.; Mkpa, E.O.; Saturday, S.A. Optimization of Hot Mix Asphalt Using Diesel Engine Waste Oil and Reclaimed Asphalt Pavement to Improve Stability and Durability. *Asian J. Eng. Appl. Technol.* **2024**, *13*, 7–14. [CrossRef]
8. Callegari, A.; Capodaglio, A. Properties and Beneficial Uses of (Bio)Chars, with Special Attention to Products from Sewage Sludge Pyrolysis. *Resources* **2018**, *7*, 20. [CrossRef]

9. Kumar, A.; Choudhary, R.; Kumar, A. Evaluation of Waste Tire Pyrolytic Oil as a Rejuvenation Agent for Unmodified, Polymer-Modified, and Rubber-Modified Aged Asphalt Binders. *J. Mater. Civ. Eng.* **2022**, *34*, 04022246. [CrossRef]
10. Hunicz, J.; Rybak, A.; Szpica, D.; Gęca, M.S.; Woś, P.; Yang, L.; Mikulski, M. Waste plastic pyrolysis oils as diesel fuel blending components: Detailed analysis of combustion and emissions sensitivity to engine control parameters. *Energy* **2024**, *313*, 134093. [CrossRef]
11. Kalampokis, S.; Manthos, E.; Konstantinidis, A.; Kakafikas, C.; Kalapouti, A. Bio-Modified Bitumen: A Comparative Analysis of Algae Influence on Characteristic Properties. *Eng* **2024**, *5*, 417–432. [CrossRef]
12. Lodi, L. Development of a sustainable circular economy system in the roofing and geo composites industries. Master's Thesis, Politecnico di Torino, Torino, Italy, 2023.
13. Li, W.; Yao, H.; Yang, D.; Peng, C.; Wang, H.; Chen, Z.; Zhao, Y. Study on Pavement Performance of Recycled Asphalt Mixture Modified by Carbon Nanotubes and Waste Engine Oil. *Appl. Sci.* **2023**, *13*, 10287. [CrossRef]
14. Jain, S. Performance and environmental evaluation of recycled mixtures consisting of waste cooking oil as a rejuvenator. *Int. J. Pavement Eng.* **2025**, *26*, 2544896. [CrossRef]
15. Bilema, M.; Aman, M.Y.; Hassan, N.A.; Memon, Z.A.; Omar, H.A.; Yusoff, N.I.M.; Milad, A. Mechanical performance of reclaimed asphalt pavement modified with waste frying oil and crumb rubber. *Materials* **2021**, *14*, 2781. [CrossRef] [PubMed]
16. Khan, M.Z.H.; Koting, S.; Katman, H.Y.B.; Ibrahim, M.R.; Babalghaith, A.M.; Asqool, O. Performance of High Content Reclaimed Asphalt Pavement (RAP) in Asphaltic Mix with Crumb Rubber Modifier and Waste Engine Oil as Rejuvenator. *Appl. Sci.* **2021**, *11*, 5226. [CrossRef]
17. Zhao, Y.; Chen, M.; Wu, S.; Zhu, Y.; Zhou, X.; Yang, C.; Zhao, Z.; Zhang, J.; Chen, D. Feasibility assessment of palmitamide derived from waste edible oil as a warm mix asphalt additive. *Constr. Build. Mater.* **2023**, *401*, 132972. [CrossRef]
18. Jain, S.; Chandrappa, A.K. Investigation on blending characteristics in asphalt mixtures with recycled asphalt and waste cooking oil as rejuvenator. *Int. J. Pavement Eng.* **2023**, *24*, 2253966. [CrossRef]
19. Liu, F.; Liu, P.; Zhang, X.; Zhou, Z.; Peng, Y. Effect of re-aging on chemical and rheological properties of waste engine oil rejuvenated asphalt binder. *Constr. Build. Mater.* **2023**, *408*, 133798. [CrossRef]
20. Tushar, Q.; Santos, J.; Zhang, G.; Robert, D.; Giustozzi, F. Recycled used cooking oil (UCO) as a rejuvenator in high content reclaimed asphalt pavement (RAP) mixes: A life cycle assessment (LCA). *Sci. Total Environ.* **2025**, *961*, 178376. [CrossRef] [PubMed]
21. *AASHTO M. 320*; Standard Specification for Performance-Graded Asphalt Binder. AASHTO: Washington, DC, USA, 2023.
22. *AASHTO T. 315*; Standard Method of Test for Determining the Rheological Properties of Asphalt Binder Using a Dynamic Shear Rheometer (DSR). American Association of State Highway and Transportation Officials (AASHTO): Washington, DC, USA, 2022.
23. *AASHTO T. 313*; Standard Method of Test for Determining the Flexural Creep Stiffness of Asphalt Binder Using the Bending Beam Rheometer (BBR). American Association of State Highway and Transportation Officials (AASHTO): Washington, DC, USA, 2022.
24. *AASHTO T316*; Standard method of test for viscosity determination of asphalt binder using rotational viscometer. American Association of State Highway and Transportation Officials: Washington, DC, USA, 2022.
25. *AASHTO T 48*; Standard Method of Test for Flash Point of Asphalt Binder by Cleveland Open Cup. American Association of State Highway and Transportation Officials (AASHTO): Washington, DC, USA, 2022.
26. *AASHTO T 44*; Standard Method of Test for Solubility of Bituminous Materials in Organic Solvents. American Association of State Highway and Transportation Officials (AASHTO): Washington, DC, USA, 2022.
27. Obaid, H.A.; Hashim, T.M.; Al-Abody, A.A.M.; Nasr, M.S.; Abbas, G.H.; Kadhim, A.M.; Sadique, M. Properties of Modified Warm-Mix Asphalt Mixtures Containing Different Percentages of Reclaimed Asphalt Pavement. *Energies* **2022**, *15*, 7813. [CrossRef]
28. *ASTM C127*; Standard Test Method for Relative Density (Specific Gravity) and Absorption of Coarse Aggregate. ASTM International: West Conshohocken, PA, USA, 2020.
29. *ASTM C131/C131M*; Standard Test Method for Resistance to Degradation of Small-Size Coarse Aggregate by Abrasion and Impact in the Los Angeles Machine. ASTM International: West Conshohocken, PA, USA, 2020.
30. *ASTM D4791*; Standard Test Method for Flat Particles, Elongated Particles, or Flat and Elongated Particles in Coarse Aggregate. The American Society of the International Association for Testing and Materials: West Conshohocken, PA, USA, 2011.
31. *ASTM C128*; Standard Test Method for Relative Density (Specific Gravity) and Absorption of Fine Aggregate. ASTM International: West Conshohocken, PA, USA, 2020.
32. *ASTM D2419*; Standard Test Method for Sand Equivalent Value of soils and Fine Aggregate. ASTM International: West Conshohocken, PA, USA, 2022.
33. *ASTM C136-06*; Standard Test Method for Sieve Analysis of Fine and Coarse Aggregates. ASTM International: West Conshohocken, PA, USA, 2006.
34. Al-Khafaji, F.F.; Kadhim, A.; Hashim, T.M. Advanced Sustainable Pavement: Eco-Friendly Stone Matrix Asphalt Engineered with Recycled Additives. *Open Civ. Eng. J.* **2026**, *20*. [CrossRef]
35. *ASTM C188*; Standard Test Method for Density of Hydraulic Cement. ASTM International: West Conshohocken, PA, USA, 2020.

36. *ASTM C204*; Standard Test Methods for Fineness of Hydraulic Cement by Air-Permeability Apparatus. ASTM International: West Conshohocken, PA, USA, 2020.
37. Yu, S.; Li, P.; Zhang, Z.; Shen, S. Virgin Binder Determination for High RAP Content Mixture Design. *J. Mater. Civ. Eng.* **2021**, *33*, 04021112. [CrossRef]
38. *AASHTO T 164/T 319*; Standard Method of Test for Quantitative Extraction of Asphalt Binder from Hot Mix Asphalt (HMA); Standard Method of Test for Quantitative Determination of Asphalt Binder Content of Hot Mix Asphalt (HMA) by the Ignition Method. American Association of State Highway and Transportation Officials: Washington, DC, USA, 2022.
39. *AASHTO T 164*; Standard Method of Test for Quantitative Extraction of Asphalt Binder from Hot Mix Asphalt (HMA). American Association of State Highway and Transportation Officials (AASHTO): Washington, DC, USA, 2022.
40. *AASHTO T 49*; Standard Method of Test for Penetration of Bituminous Materials. American Association of State Highway and Transportation Officials (AASHTO): Washington, DC, USA, 2022.
41. *AASHTO T 53*; Standard Method of Test for Softening Point of Bitumen (Ring-and-Ball Apparatus). American Association of State Highway and Transportation Officials: Washington, DC, USA, 2022.
42. *AASHTO T 84/T 85*; Standard Method of Test for Specific Gravity and Absorption of Fine Aggregate. American Association of State Highway and Transportation Officials: Washington, DC, USA, 2022.
43. *AASHTO T 27/T 11*; Standard Method of Test for Sieve Analysis of Fine and Coarse Aggregates; Standard Method of Test for Materials Finer than 75-µm (No. 200) Sieve in Mineral Aggregates by Washing. American Association of State Highway and Transportation Officials: Washington, DC, USA, 2022.
44. *AASHTO T 96*; Standard Method of Test for Resistance to Degradation of Small-Size Coarse Aggregate by Abrasion and Impact in the Los Angeles Machine. American Association of State Highway and Transportation Officials: Washington, DC, USA, 2022.
45. *AASHTO T 176*; Standard Method of Test for Plastic Fines in Graded Aggregates and Soils by Use of the Sand Equivalent Test. American Association of State Highway and Transportation Officials: Washington, DC, USA, 2022.
46. AL Sa'adi, A.H.; Al-Khafaji, F.F.; Hashim, T.M.; Hussein, M.L.; Ali, Y.A.; Ali, A.H.; Jebur, Y.M.; Ali, L.H.; Al-Mulali, M.Z.; Al-Khazraji, A.A. Prospect of using geotextile reinforcement within flexible pavement layers to reduce the effects of rutting in the middle and southern parts of Iraq. *J. Mech. Behav. Mater.* **2022**, *31*, 323–336. [CrossRef]
47. *ASTM D4052*; Standard Test Method for Density, Relative Density, and API Gravity of Liquids by Digital Density Meter. ASTM International: West Conshohocken, PA, USA, 2018.
48. *ASTM D445-12*; Standard Test Method for Kinematic Viscosity of Transparent and Opaque Liquids (and Calculation of Dynamic Viscosity). ASTM International: West Conshohocken, PA, USA, 2012.
49. *ASTM D92*; Standard Test Method for Flash and Fire Points by Cleveland Open Cup Tester. ASTM International: West Conshohocken, PA, USA, 2020.
50. *ASTM D97*; Standard Test Method for Pour Point of Petroleum Products. ASTM International: West Conshohocken, PA, USA, 2020.
51. *ASTM D95*; Standard Test Method for Water in Petroleum Products and Bituminous Materials by Distillation. ASTM International: West Conshohocken, PA, USA, 2020.
52. *AASHTO R 35*; Standard Practice for Superpave Volumetric Design for Asphalt Mixtures. American Association of State Highway and Transportation Officials: Washington, DC, USA, 2022.
53. Sreeram, A.; Leng, Z.; Hajj, R.; Ferreira, W.L.G.; Tan, Z.; Bhasin, A. Fundamental investigation of the interaction mechanism between new and aged binders in binder blends. *Int. J. Pavement Eng.* **2020**, *23*, 1317–1327. [CrossRef]
54. *AASHTO T 312*; Standard Method of Test for Preparing and Determining the Density of Hot Mix Asphalt (HMA) Specimens by Means of the Superpave Gyratory Compactor. American Association of State Highway and Transportation Officials: Washington, DC, USA, 2022.
55. *AASHTO M 323*; Standard Specification for Superpave Volumetric Mix Design. American Association of State Highway and Transportation Officials: Washington, DC, USA, 2022.
56. *AASHTO T 324*; Standard Method of Test for Hamburg Wheel-Track Testing of Compacted Hot Mix Asphalt (HMA). American Association of State Highway and Transportation Officials: Washington, DC, USA, 2022.
57. Al-Khafaji, F.F.; Hashim, T.M. Revolutionizing Self-Healing Asphalt: Optimized Encapsulated Rejuvenators for Enhanced Durability and Sustainability. *Civ. Eng. J.* **2025**, *11*, 2826–2839. [CrossRef]
58. *AASHTO TP 125*; Standard Method of Test for Determining the Flexibility Index of Asphalt Mixtures Using the Illinois Flexibility Index Test (I-FIT). American Association of State Highway and Transportation Officials: Washington, DC, USA, 2022.
59. *ASTM D8225*; Standard Test Method for In-Place Determination of Asphalt Pavement Density Using an Electromagnetic Asphalt Density Gauge. ASTM International: West Conshohocken, PA, USA, 2020.
60. Khan, M.Z.H. Performance Characteristics of Crumb Rubber Modified Asphalt Mixed with Reclaimed Asphalt Pavement and Waste Engine Oil. Master's Thesis, University of Malaya, Kuala Lumpur, Malaysia, 2022.

61. Rafiq, W.; Bin Napiah, M.; Hartadi Sutanto, M.; Salah Alaloul, W.; Nadia Binti Zabri, Z.; Imran Khan, M.; Ali Musarat, M. Investigation on Hamburg Wheel-Tracking Device Stripping Performance Properties of Recycled Hot-Mix Asphalt Mixtures. *Materials* **2020**, *13*, 4704. [CrossRef] [PubMed]
62. Saed, S.A.; Ziari, H.; Kamboozia, N.; Dehaghi, E.A. Rheological and aging performance of reclaimed asphalt binders modified by warm mix additive and recycling agent. *Sci. Rep.* **2025**, *15*, 44697. [CrossRef] [PubMed]